

Phase Diagrams and Thermodynamic Properties of Binary Systems of Drugs

James Sangster^{a)}

Sangster Research Laboratories, Suite 402, 3475 de la Montagne, Montreal, Quebec H3G 2A4, Canada

Received December 1, 1998; revised manuscript received February 19, 1999

The phase diagram data of 60 binary systems of drugs were evaluated with the aid of a computer-coupled phase diagram/thermodynamic analysis. Data for this analysis were obtained by an exhaustive literature search (110 references). Among the results of this analysis are the excess Gibbs energy of liquid and solid solution phases, and the thermodynamic properties of intermediate compounds. For each system a phase diagram was calculated; such calculated diagrams are thermodynamically consistent and are offered as the best constructions which can be deduced from available data. © 1999 American Institute of Physics and American Chemical Society. [S0047-2689(99)00303-7]

Key words: phase diagrams; thermodynamic properties.

Contents

1. Introduction.....	891	(B).....	902
2. Thermodynamic Analysis of Phase Diagrams....	891	12.12. Aminophenazone (A)+Phenazone (B).....	902
3. Computer-Coupled Phase Diagram/ Thermodynamic Analysis.....	891	12.13. Thiourea (A)+Aminophenazone (B).....	902
4. Solid Solutions of Limited Solubility.....	891	12.14. Urea (A)+Aminophenazone (B).....	903
5. Experimental Methods of Measurement.....	892	12.15. Aminophenazone (A)+Allobarbitol (B)....	904
6. Polymorphism and Metastable States.....	892	12.16. Aminophenazone (A)+Barbital (B).....	905
7. Retrieval and Treatment of Data.....	892	12.17. Aminophenazone (A)+Sulfisoxazole (B)..	905
8. Properties of the Pure Substances.....	892	12.18. 3-Methoxybenzoic Acid (A)+Etofylline (B).....	905
9. Estimation of Enthalpy of Fusion.....	895	12.19. Benzoic Acid (A)+Etofylline (B).....	906
10. Temperature Dependence of Enthalpy of Fusion.....	895	12.20. Aminophenazone (A)+Etofylline (B).....	906
11. Thermodynamic Analysis and Presentation of Results.....	896	12.21. 4-Nitroaniline (A)+Etofylline (B).....	907
12. Analysis of Phase Diagrams.....	897	12.22. Benzidine (A)+Etofylline (B).....	908
12.1. Phenazone (A)+Phenylbutazone (B).....	897	12.23. Hydroquinone (A)+Etofylline (B).....	908
12.2. Phenazone (A)+Phenacetin (B).....	897	12.24. 4-Nitrophenol (A)+Etofylline (B).....	909
12.3. Phenazone (A)+Urea (B).....	898	12.25. Phenacetin (A)+Urea (B).....	910
12.4. Paracetamol (A)+Phenazone (B).....	898	12.26. Acetanilide (A)+Phenacetin (B).....	910
12.5. Sulfadiazine (A)+Trimethoprim (B).....	899	12.27. Phcnacctin (A) + Phcnobarbital (B).....	911
12.6. Sulfamethoxazole (A)+Trimethoprim (B).....	899	12.28. Paracetamol (A)+Phenobarbital (B).....	911
12.7. Benzoic Acid (A)+Trimethoprim (B).....	900	12.29. Urea (A)+Phenobarbital (B).....	912
12.8. Sulfamethoxyipyridazine (A)+Trimethoprim (B).....	900	12.30. Theophylline (A)+Phenobarbital (B).....	913
12.9. Aminophenazone (A)+4-Aminophenazone (B).....	901	12.31. Quinine (A)+Phenobarbital (B).....	913
12.10. Aminophenazone (A)+Phenacetin (B)....	901	12.32. Caffeine (A)+Phenobarbital (B).....	914
12.11. Aminophenazone (A)+Phenylbutazone (B).....	902	12.33. Aspirin (A)+Phenobarbital (B).....	914
		12.34. Sulfanilamide (A)+Phenylbutazone (B)...	915
		12.35. Khellin (A)+Sulfanilamide (B).....	915
		12.36. Sulfanilamide (A)+Benzocaine (B).....	916
		12.37. Sulfanilamide (A)+4-Aminobenzoic Acid (B).....	916
		12.38. Caffeine (A)+Sulfathiazole (B).....	917
		12.39. Sulfathiazole (A)+Phenylbutazone (B)....	917
		12.40. Phenazone (A)+Sulfathiazole (B).....	918
		12.41. Sulfathiazole (A)+Benzocaine (B).....	919
		12.42. Sulfathiazole (A)+4-Aminobenzoic Acid (B).....	919
		12.43. Nicotinamide (A)+Theophylline (B).....	920

^{a)}Electronic mail: jsangster@mail.polymtl.ca

©1999 by the U.S. Secretary of Commerce on behalf of the United States. All rights reserved. This copyright is assigned to the American Institute of Physics and the American Chemical Society. Reprints available from ACS; see Reprints List at back of issue.

12.44. Nicotinamide (A)+Indomethacin (B).	920
12.45. Nicotinamide (A)+Sulfamerazine (B).	921
12.46. Khellin (A)+Sulfapyridine (B).	922
12.47. Khellin (A)+Nicotinic Acid (B).	923
12.48. Urea (A)+Khellin (B).	923
12.49. Khellin (A)+Caffeine (B).	923
12.50. Khellin (A)+Nicotinamide (B).	923
12.51. Khellin (A)+Sulfacetamide (B).	924
12.52. Theophylline (A)+Paracetamol (B).	925
12.53. Caffeine (A)+Paracetamol (B).	925
12.54. 4-Aminobenzoic Acid (A)+Caffeine (B).	926
12.55. Anthranilic Acid (A)+Caffeine (B).	926
12.56. Benzoic Acid (A)+Isonicotinamide (B).	927
12.57. 2-Nitroaniline (A)+4-Aminobenzoic Acid (B).	928
12.58. Succinimide (A)+Urea (B).	928
12.59. Chlormadinone Acetate (A)+Ethinyl Estradiol (B).	929
12.60. Estradiol Benzoate (A)+Estradiol Phenylpropionate (B).	929
13. Acknowledgments.	929
14. References.	929

List of Tables

1. Melting points and fusion properties of the pure components.	893
2. The temperature dependence of the enthalpy and entropy of fusion of benzocaine.	896

List of Figures

1. The system phenazone (A)+phenylbutazone (B).	896
2. The system phenazone (A)+phenacetin (B).	897
3. The system phenazone (A)+urea (B).	897
4. The system paracetamol (A)+phenazone (B).	898
5. The system sulfadiazine (A)+trimethoprim (B).	898
6. The system sulfamethoxazole (A)+trimethoprim (B).	899
7. The system benzoic acid (A)+trimethoprim (B).	899
8. The system sulfamethoxy pyridazine (A)+trimethoprim (B).	900
9. The system aminophenazone (A)+4-aminophenazone (B).	901
10. The system aminophenazone (A)+phenacetin (B).	901
11. The system aminophenazone (A)+phenylbutazone A(B).	902
12. The system aminophenazone (A)+phenazone (B).	902
13. The system thiourea (A)+aminophenazone (B).	903
14. The system urea (A)+aminophenazone (B). Part of the diagram is conjectural.	903
15. The system aminophenazone (A)+allobarbitol (B).	904
16. The system aminophenazone (A)+barbitol (B).	904
17. The system aminophenazone (A)+sulfisoxazole (B).	905
18. The system 3-methoxybenzoic acid (A)+etofylline (B).	906
19. The system benzoic acid (A)+etofylline (B).	906
20. The system aminophenazone (A)+etofylline (B).	907
21. The system 4-nitroaniline (A)+etofylline (B).	907
22. The system benzidine (A)+etofylline (B).	908
23. The system hydroquinone (A)+etofylline (B).	908
24. The system 4-nitroenol (A)+etofylline (B).	909
25. The system phenacetin (A)+urea (B). The calculated immiscibility envelope is conjectural.	909
26. (a) The system acetanilide (A)+phenacetin (B). possible interpretation of the data. (b). The system acetanilide (A)+phenacetin (B). Another possible interpretation of the data.	910
27. The system phenacetin (A)+phenobarbital (B).	911
28. The system paracetamol (A)+phenobarbital (B).	911
29. The system urea (A)+phenobarbital (B). The diagram is conjectural.	912
30. The system theophylline (A)+phenobarbital (B).	912
31. The system quinine (A)+phenobarbital (B).	913
32. The system caffeine (A)+phenobarbital (B).	914
33. The system aspirin (A)+phenobarbital (B).	914
34. The system sulfanilamide (A)+phenylbutazone (B).	915
35. The system khellin (A)+sulfanilamide (B).	915
36. The system sulfanilamide (A)+benzocaine (B).	916
37. The system sulfanilamide (A)+4-aminobenzoic acid (B).	916
38. The system caffeine (A)+sulfathiazole (B).	917
39. The system sulfathiazole (A)+phenylbutazone (B).	917
40. The system phenazone (A)+sulfathiazole (B).	918
41. The system sulfathiazole (A)+benzocaine (B).	918
42. The system sulfathiazole (A)+4-aminobenzoic acid (B).	919
43. The system nicotinamide (A)+theophylline (B).	919
44. The system nicotinamide (A)+indomethacin (B). Most of the diagram is conjectural.	920
45. The system nicotinamide (A)+sulfamerazine (B).	920
46. The system khellin (A)+sulfapyridine (B).	921
47. The system khellin (A)+nicotinic acid (B).	921
48. The system urea (A)+khellin (B).	922
49. The system khellin (A)+caffeine (B).	922
50. The system khellin (A)+nicotinamide (B).	923
51. The system khellin (A)+sulfacetamide (B).	924
52. The system theophylline (A)+paracetamol (B).	924
53. The system caffeine (A)+paracetamol (B).	925
54. The system 4-aminobenzoic acid (A)+caffeine (B).	925
55. The system anthranilic acid (A)+caffeine (B).	926
56. The system benzoic acid (A)+isonicotinamide (B). The existence of the 2:1 compound is debatable.	926
57. The system 2-nitroaniline (A)+4-aminobenzoic	

acid (B).....	927
58. The system succinimide (A)+urea (B).....	927
59. The system chlormadinone acetate (A)+ethinyl estradiol (B).....	928
60. The system estradiol benzoate (A)+estradiol phenylpropionate (B).....	928

1. Introduction

The biological activity of medicinal chemicals is a proper concern of health professionals and the pharmaceutical industry. This includes interactions between different substances simultaneously present in vivo. Many drugs are manufactured in solid tablet form, in which case crystal structure can influence tableting ability¹ and dissolution behavior.² Since many drugs can persist in one or more metastable solid modifications (polymorphism³), the properties of these metastable forms also are important for predicting stability in storage. When two compounds are combined in solid form it is prudent to be aware of interactions in the solid state which may affect the final efficacy of the preparation.⁴

In the tableting operation, pressure is applied to the solid mass, whose temperature may rise to a variable degree. If the two compounds form a simple eutectic, the physical mixture of eutectic composition may have properties different from those of a fused mass.⁵ If an intermediate compound is formed, its stability must be ascertained.⁶ The complex, upon ingestion, may or may not decompose to give the original components⁷ and the complex itself may have pharmaceutical properties different from its component drugs.⁸⁻¹⁰ The formation of a solid solution between a difficultly soluble substance and another drug may ameliorate the dissolution properties of the difficultly soluble compound.^{11,12}

A number of methods have been used to investigate interactions between drug molecules in the solid state. Among them are: x-ray diffraction, absorption spectrophotometry [ultraviolet (UV), infrared (IR)], thermogravimetric analysis, refractive index and differential thermal analysis^{3,13} (DTA). When applied to a binary drug system, DTA and differential scanning calorimetry (DSC) enable the phase diagram of the system to be obtained, including the following properties:

- (i) melting points and enthalpy of fusion of pure substances, eutectics and intermediate compounds
- (ii) determination of drug purity,¹⁴
- (iii) polymorphism,
- (iv) thermal stability,
- (v) glass transitions, and
- (vi) solid solubility.

2. Thermodynamic Analysis of Phase Diagrams

Although a number of binary phase diagrams of pharmaceutical substances have been measured and reported, both the quantity and quality of the data are highly variable. The experimental methods used have different strengths and weaknesses, and the reported phase diagrams are not always

consistent with thermodynamic constraints arising from the condition of equilibrium. In the present work, a computer-coupled phase diagram/thermodynamic analysis was used to calculate a phase diagram for each of 60 systems examined. This type of analysis uses available phase diagram and thermodynamic constraints and effects a correct thermodynamic smoothing of experimental data. Other results of this analysis include the deduction of excess Gibbs energies of solution phases and thermodynamic properties of intermediate compounds. The procedure has been applied with equal success to systems of molten salts,¹⁵ organic compounds,^{16,17} metal oxides¹⁸ and liquid crystals.¹⁹

3. Computer-Coupled Phase Diagram/ Thermodynamic Analysis

The thermodynamic basis of phase diagrams is well known.^{20,21} The analysis used here has been described previously;^{15,17} the principal features are summarized in what follows. The given data are those of the pure components and the liquidus, solidus, eutectic and peritectic temperature arrests. The computer program performs a simultaneous least-squares optimization of the thermodynamic and phase diagram data, resulting in expressions for the excess Gibbs energies of liquid and solid solution phases and thermodynamic properties of intermediate compounds (if any). With these data, a phase diagram is calculated and the invariant points of the system are deduced. The computer programs are available on-line²² and also on microcomputer diskette (details available from the author).

4. Solid Solutions of Limited Solubility

As a general rule, systems of organic compounds do not exhibit solid solubility, principally because the crystalline structures of the components are usually incompatible. When there is no solid solution, the limiting liquidus slope near a pure component (say A) is given by^{15,17}

$$(dx_A/dT)_{\text{liq}} = \Delta_{\text{fus}}H_A / RT_{\text{fus}}^2, \quad (1)$$

where T_{fus} is the melting point of component A and $\Delta_{\text{fus}}H_A$ is the enthalpy of fusion. The expression on the right hand side (RHS) is simply the reciprocal of the well-known freezing point depression constant and depends only on properties of the solvent. A similar expression holds for the other component. Equation (1) is useful in preliminary analysis of phase diagram data in suggesting the presence or absence of solid solubility or in the critical evaluation of experimental liquidus data.¹⁷ Equation (1) is a necessary thermodynamic requirement for equilibrium phase diagrams, and all phase diagrams shown in the present work adhere to this constraint.

In a few cases, solid solubility was included in the phase diagram in order to reproduce the experimental liquidus. The solid solution was assumed to be Henrian, i.e., the activity of the solvent was assumed to be unity and the solute was rep-

resented by a temperature-independent activity coefficient.^{15,17} In actuality, of course, these are approximations, but suffice for the purposes at hand.

5. Experimental Methods of Measurement

Various techniques were used to determine phase diagrams for the systems studied:

- (1) thermal analysis (cooling curves),
- (2) thaw-melt method,
- (3) DTA, DSC,
- (4) Kofler's contact (microthermal) method,
- (5) hot-stage microscope, and
- (6) light transmission.

All these are methods for detecting the solid-liquid phase change as a function of temperature and composition. Methods 1-5 have been described and evaluated.^{4,17,21} In method 6, the phase change is registered automatically by the response of a photocell to transmitted light.

In the evaluation of phase diagram data from these methods, several considerations are pertinent:

- (i) supercooling,
- (ii) use of heating or cooling mode,
- (iii) visual or instrumental detection, and
- (iv) preparation of mixtures.

The same system, studied by different methods, may yield rather different results.⁴ In the present work, experimental methods are stated in the discussion of every system and mention of experimental peculiarities is made and accounted for. Other supplementary experimental methods were: x-ray diffraction, microphotographic analysis and IR spectroscopy. Their purpose was generally to confirm features of the solid state (solid solutions, presence of compounds, etc.).

6. Polymorphism and Metastable States

Drugs, being organic compounds, may exist in one or more metastable solid states, in addition to the thermodynamically stable one.^{3,23} These states require a change of crystal structure in the solid in order to be transformed and in practice can persist for appreciable periods. Their melting points are often quite close to that of the stable form; these properties are potentially complicating factors in the interpretation of the results of thermal methods. Since their appearance and persistence are reproducible, experimental conditions can be established to minimize their effects. The phase diagrams considered in the present work deal only with thermodynamically stable states.

The method of preparation of samples for analysis by thermal methods has been found to be important for the establishment of an equilibrium phase diagram. For example, physical mixtures—however finely divided—showed metastable eutectics in thermal analytical methods. Prefused mixtures prepared by solvent evaporation were found to give more reproducible results. In the present work, only stable

features are reproduced in phase diagrams, but experimental metastable ones are mentioned whenever they were reported.

It should be emphasized here that the effects of polymorphism in drug compounds are of great importance to pharmaceutical chemists, for evident practical reasons. The present analysis is limited to thermodynamically stable states because inclusion of metastable states would greatly enlarge the article and obscure the application of fundamental thermodynamic relationships.

7. Retrieval and Treatment of Data

Apart from Chemical Abstracts, some compilations^{13,23,24} were useful in locating phase diagram data. Where the data were not tabulated, they were read off the published phase diagrams. Both liquidus and solidus data were retrieved, and are shown on the calculated phase diagrams. In general, eutectic data and congruent melting points of compounds were given somewhat more weight than other liquidus data in the optimization step, for stated reasons.¹⁷ Where the data were sparse or contradictory, some prior decisions were made concerning the general shape or features of the phase diagram. These preliminary steps are explained in the evaluations of individual systems.

It is pertinent to add that the choice of systems examined was governed principally by the existence of phase diagram data amenable to a thermodynamic analysis of the present type. The phase diagrams are illustrative but not meant to be "representative" of any particular area of inquiry in pharmaceutical chemistry.

8. Properties of the Pure Substances

Evaluations of the present type require reliable data for melting points and enthalpies of fusion of the pure components. There are standard handbooks of melting points;^{3,25-29} information from these will be referred to henceforth as "handbook data." For enthalpies of fusion, two sources were generally useful.^{30,31} In addition to these sources, melting point and enthalpy of fusion data were retrieved from individual articles; these are mentioned below for each substance considered.

Table 1 presents the data adopted in the present work. Temperatures are quoted to the nearest 0.1 °C, irrespective of source, since the precision of experimental phase diagram data does not warrant citation of hundredths of a degree. For similar reasons, only three significant figures were retained for enthalpies of fusion. The larger number of significant figures given for the entropy of fusion were used for accurate reproduction of adopted melting points; they have no further significance. In what follows, the given name of the drug is accompanied, in square brackets, by other information: formula, Chemical Abstracts Registry Number and other informal names (if any).

Acetanilide [C_8H_9NO ; 103-84-4; Acetamide, N-phenyl-]. The enthalpy of fusion was reported to be³² 20.5 or^{30,33,34}

TABLE 1. Melting points and fusion properties of the pure compounds^a

Name	$T_{\text{fus}}, ^\circ\text{C}$	$\Delta_{\text{fus}}H, \text{kJ mol}^{-1}$	$\Delta_{\text{fus}}S, \text{J mol}^{-1} \text{K}^{-1}$
Acetanilide	114.3	21.3	54.968
Allobarbitol	173.0	32.3	72.389
4-Aminobenzoic acid	188.2	22.5	48.765
Aminophenazone	107.5	27.6	72.498
4-Aminophenazone	108.3	24.9	65.269
Anthranilic acid	145.4	20.5	48.973
Aspirin	135.0	(27.2)	(66.634)
Barbital	189.6	24.7	53.371
Benzidine	127.0	19.1	47.726
Benzocaine	89.7	22.3	61.449
Benzoic acid	122.4	17.6	44.489
Caffeine	236.3	22.0	43.180
Chlormadinone acetate	211.7	(27.3)	(56.300)
Estradiol benzoate	192.4	41.8	89.777
Estradiol phenylpropionate	127.2	33.0	82.418
Ethinyl estradiol	183.5	27.9	61.090
Etofylline	160.6	(29.6)	(68.234)
Hydroquinone	172.3	27.1	60.831
Indomethacin	160.3	36.9	85.121
Isonicotinamide	157.2	(24.8)	(57.628)
Khellin	153.4	32.3	75.715
3-Methoxybenzoic acid	110.5	(23.8)	(62.028)
Nicotinamide	129.3	23.2	57.640
Nicotinic acid	237.3	(27.9)	(54.652)
2-Nitroaniline	72.0	16.1	46.640
4-Nitroaniline	147.5	21.1	50.155
4-Nitrophenol	113.8	18.3	47.287
Paracetamol	169.3	30.5	68.927
Phenacetin	134.2	33.0	81.001
Phenazone	110.6	27.3	71.131
Phenobarbital	175.0	27.8	62.026
Phenylbutazone	105.6	27.7	73.126
Quinine	176.3	(22.9)	(50.945)
Succinimide	123.2	(25.1)	(63.320)
Sulfacetamide	183.9	22.4	49.005
Sulfadiazine	257.8	42.6	80.226
Sulfamerazine	236.3	38.7	75.957
Sulfamethoxazole	169.8	32.2	72.686
Sulfamethoxypyridazine	180.9	31.3	68.928
Sulfanilamide	165.0	(26.5)	(60.475)
Sulfapyridine	191.3	34.4	74.058
Sulfathiazole	201.0	26.4	55.673
Sulfisoxazole	195.7	30.2	64.406
Theophylline	274.0	29.5	53.911
Thiourea	177.0	14.4	31.986
Trimethoprim	199.3	49.4	104.550
Urea	132.6	14.3	35.239

^aData in parentheses were estimated.

21.7 kJ mol⁻¹. The melting point, from handbooks, is 113–115 °C; individual determinations^{30,33–37} are close to 114 °C.

Allobarbitol [C₁₀H₁₂N₂O₃; 52-43-7; 2,4,6(1H,3H,5H) Pyrimidinetrione, 5,5-di(2-propenyl-); Diadol, Dial]. Handbook data for the melting point lie in the range 171–174 °C. The true melting point is probably³⁵ close to 173 °C. The enthalpy of fusion is³⁸ 24.9 or³⁹ 32.3 kJ mol⁻¹.

4-Aminobenzoic acid [C₇H₇NO₂; 150-13-0; PABA]. The melting range from handbooks is 187–189 °C; a value

closer to 188 °C was chosen.^{30,40} The enthalpy of fusion was reported^{30,40} as 20.9 or⁴¹ 24.0 kJ mol⁻¹.

Aminophenazone [C₁₃H₁₇N₃O; 58-15-1; Pyrazole-3-one, 4-(dimethylamino)-1,2-dihydro-1,5-dimethyl-2-phenyl-; aminopyrine, amidopyrine]. The handbook melting point is 107–109 °C, and a value^{37,42–44} between 107 and 108 °C was chosen. There is one value for the enthalpy of fusion.⁴⁵

4-Aminophenazone [C₁₁H₁₃N₃O; 83-07-8; 3H-Pyrazol-3-one, 4-amino-1,2-dihydro-1,5-dimethyl-2-phenyl-]. Handbooks give 109 °C as the melting point, but individual reports^{35,42,45,46} indicate a temperature closer to 108 °C. There is one value for the enthalpy of fusion.⁴⁵

Anthranilic acid [C₇H₇NO₂; 118-92-3; Benzoic acid, 2-amino-]. The handbook melting range is 144–148 °C. A melting point in the lower range^{30,40} was chosen. The enthalpy of fusion is the mean of two values.^{30,40}

Aspirin [C₉H₈O₄; 50-78-2; Benzoic acid, 2-(acetyloxy)-; Acetylsalicylic acid]. The handbook melting point is 135 °C, although the freezing point is often quoted to be much lower. This was taken to be the correct value.^{4,47} There is no experimental value for the enthalpy of fusion, and so it was estimated (next section).

Barbital [C₈H₁₂N₂O₃; 57-44-3; 2,4,6(1H,3H,5H)-Pyrimidinetrione, 5,5-diethyl-; Veronal, Barbitone]. The handbook melting range is 188–192 °C, and the adopted value^{3,5,48} is close to 190 °C. The enthalpy of fusion is³⁸ 24.4 or³⁹ 25.0 kJ mol⁻¹.

Benzidine [C₁₂H₁₂N₂; 92-87-5; [1,1'-Biphenyl]-4,4'-diamine]. The handbook melting point is 128 °C, and the adopted value is from a phase diagram study.⁴⁹ The enthalpy of fusion, from the same source, is 19.1 kJ mol⁻¹.

Benzocaine [C₉H₁₁O₂; 94-09-7; Benzoic acid, 4-amino-, ethyl ester; Parathesin]. The melting range from handbook sources is 88–92 °C. A more accurate value is close^{32,40,50} to 90 °C. The enthalpy of fusion lies in the range^{32,40,50} 22.0–23.6 kJ mol⁻¹.

Benzoic acid [C₇H₆O₂; 65-85-0]. The chosen melting point^{30,40,51} is close to the handbook value. The enthalpy of fusion is the mean of several determinations.^{30,40,51,52}

Caffeine [C₈H₁₀N₄O₂; 58-08-2; 1H-Purine-2,6-dione, 3,7-dihydro-1,3,7-trimethyl-]. Handbook data for the melting point lie in the range 235–238 °C. A temperature near 236 °C was adopted.^{30,35} The enthalpy of fusion^{30,32,53} values are 21.0–27.7 kJ mol⁻¹.

Chlormadinone acetate [C₂₃H₂₉ClO₄; 302-22-7; Progna-4,6-diene-3,20-dione, 17(acetyloxy)-6-chloro-]. Handbooks indicate 212–214 °C as the melting point. The adopted value was taken from a recent phase diagram study.⁵⁴ Since there is no experimental value for the enthalpy of fusion it was estimated (next section).

Estradiol benzoate [C₂₅H₂₈O₃; 50-50-0; Estra-1,3,5(10)-triene-3,7-diol (17 β), 3-benzoate; Benztrone]. Handbook melting point data indicate 188–196 °C, and a value close to 192 °C was adopted.^{55,56} The enthalpy of fusion is³² 35.9 or⁵⁵ 41.8 kJ mol⁻¹.

Estradiol phenylpropionate [C₂₇H₃₂O₃; 28572-75-0; Estra-1,3,5(10)-triene-3,7-diol (17 β), 3-(3-phenylpropionate)].

Handbook melting point data give 126–128 °C, and the adopted value is a mean from two sources.^{55,56} There is one value⁵⁵ for the enthalpy of fusion.

Ethinyl estradiol [C₂₀H₂₄O₂; 57-63-6; 19-Norpregna-1,3,5(10)-trien-20-yne-3,17-diol,(17 α)-]. The melting point data according to handbooks are not consistent: 145–146 °C or 182–184 °C. The higher temperature is preferred.⁵⁴ The enthalpy of fusion was reported to be^{32,54} 22.4–28.1 kJ mol⁻¹.

Etofylline [C₉H₁₂N₄O₃; 519-37-9; 1H-Purine-2,6-dione, 3,7-dihydro-7-(2-hydroxyethyl)-1,3-dimethyl-; Oxytheonyl]. The handbook melting point is 158 °C, but the value adopted is that from a phase diagram study.⁵⁷ There is no experimental value for the enthalpy of fusion, so it was estimated (next section).

Hydroquinone [C₆H₆O₂; 123-31-9; Benzene, 1,4-dihydroxy-]. The melting range is 172–179 °C according to handbooks; a more accurate value was chosen from studies on the pure compound.^{30,58,59} The enthalpy of fusion lies in the range^{30,58,60} 21.1–27.1 kJ mol⁻¹.

Indomethacin [C₁₉H₁₆ClNO₄; 53-86-1; 1H-Indole-3-acetic acid, 1-(4-chlorophenyl)-5-methoxy-2-methyl-]. The handbook melting range is 156–162 °C and the adopted value^{61,62} is close to 160 °C. The enthalpy of fusion is⁶³ 36.1 or³² 37.7 kJ mol⁻¹.

Isonicotinamide [C₆H₆N₂O; 1453-82-3; 4-Pyridinecarboxamide]. The handbook melting point is 155–156 °C, and the adopted value was taken from a phase diagram study.⁵ There is no experimental value for the enthalpy of fusion, so it was estimated (next section).

Khellin [C₁₄H₁₂O₅; 82-02-0; 5H-Furo[3,2-g][1]benzopyran-5-one, 4,9-dimethoxy-7-methyl-; Amicardine]. The handbook melting range is 153–155 °C, and the true melting point is probably the lower value.^{64–66} There is one value⁶⁵ for the enthalpy of fusion.

3-Methoxybenzoic acid [C₈H₈O₃; 586-38-9]. The handbook melting point is 110.5 °C, but the chosen value was taken from a phase diagram study.⁵⁷ The enthalpy of fusion is not known experimentally, and so it was estimated (next section).

Nicotinamide [C₆H₆N₂O; 98-92-0; 3-Pyridinecarboxamide; Niacinamide]. Handbooks indicate a melting range of 128–131 °C. The chosen value^{5,35,67,68} is close to 129 °C. The enthalpy of fusion was reported³² 22.8 or¹⁴ 23.6 kJ mol⁻¹. A value⁶⁸ of 26.1 J mol⁻¹ is probably a misprint.

Nicotinic acid [C₆H₅NO₂; 59-67-6; 3-Pyridinecarboxylic acid]. The melting range from handbooks is 236–237 °C; the chosen value was adopted from a phase diagram study.⁶⁷ The enthalpy of fusion, being unknown, was estimated (next section).

2-Nitroaniline [C₆H₆N₂O₂; 88-74-4; Benzenamine, 2-nitro-]. The experimental melting point range^{30,40,57} is 69–73 °C and the enthalpy of fusion^{30,40} is 16.1 kJ mol⁻¹.

4-Nitroaniline [C₆H₆N₂O₂; 100-01-6; Benzenamine, 4-nitro-]. The experimental^{30,40,57,69} melting range is 146–148 °C. The enthalpy of fusion³⁰ 21.1 kJ mol⁻¹.

4-Nitrophenol [C₆H₅NO₃; 100-02-7;]. The experimental³⁰ melting range is 112–114 °C. The enthalpy of fusion^{30,40,70,71} lies in the range 17.3–30.1 kJ mol⁻¹.

Paracetamol [C₈H₉NO₂; 103-90-2; Acetamide, N-(4-hydroxyphenyl)-; Acetaminophen]. Handbook data for the melting point indicate 167–171 °C. The adopted value is from careful studies on the pure substance.^{35,62,72} There is one datum for the enthalpy of fusion.¹⁴

Phenacetin [C₁₀H₁₃NO₂; 62-44-2; Acetamide, N-(4-ethoxyphenyl)-]. Handbook data for the melting point are 134–138 °C. The lower limit is probably correct.^{35–37,62,73} The enthalpy of fusion is^{32,74,75} 21.8–34.7 kJ mol⁻¹.

Phenazone [C₁₁H₁₂N₂O; 60-80-0; 3H-Pyrazol-3-one, 1,2-dihydro-1,5-dimethyl-2-phenyl-; Antipyrine]. According to handbooks, the melting range is 111–114 °C. A lower temperature was adopted.^{35,42,46} The enthalpy of fusion is the mean of two experimental values.^{32,45}

Phenobarbital [C₁₂H₁₂N₂O₃; 50-06-6; 2,4,6(1H,3H,5H)-Pyrimidinetrione, 5-ethyl-5-phenyl-; Luminal]. The melting range is given as 174–178 °C in handbooks. There is one value³⁸ for their enthalpy of fusion.

Phenylbutazone [C₁₉H₂₀N₂O₂; 50-33-9; 3,5-Pyrazolidinedione, 4-butyl-1,2-diphenyl-; Butadione]. The handbook melting range is 105–107 °C. A low value is indicated.^{76–78} The enthalpy of fusion lies in the range^{32,44,77,78} 26.2–29.7 kJ mol⁻¹.

Quinine [C₂₀H₂₄N₂O₂; 130-95-0; Cinchonon-9-ol, 6'-methoxy-, (8 α ,9R)-]. The melting range is 176–177 °C (with some decomposition), according to handbooks. There is no experimental value for the enthalpy of fusion, and so it was estimated (next section).

Succinimide [C₄H₅NO₂; 123-56-8; 2,5-Pyrrolidinedione]. The handbook data for melting indicate 125–127 °C, but a lower value was adopted on the basis of more careful work on the pure substance.^{79,80} There is no experimental value for the enthalpy of fusion, and so it was estimated (next section).

Sulfacetamide [C₈H₁₀N₂O₃S; 144-80-9; Acetamide, N-[(4-aminophenyl)sulfonyl]-]. Handbook melting point data indicate 181–184 °C, and the higher temperature was adopted.^{81,82} There is one value⁸¹ for the enthalpy of fusion.

Sulfadiazine [C₁₀H₁₀N₄O₂S; 68-35-9; Benzenesulfonamide, 4-amino-N-2-pyrimidinyl-]. The melting range according to handbooks is 252–262 °C. A value close to 258 °C was adopted.^{10,75,83} The reported enthalpy of fusion^{10,75,81,83,84} is 31.2–43.7 kJ mol⁻¹.

Sulfamerazine [C₁₁H₁₂N₄O₂S; 127-79-7; Benzenesulfonamide, 4-amino-N-(4-methyl-2-pyrimidinyl)-]. The handbook melting range is 234–238 °C, with some decomposition. A value near 236 °C was adopted.^{81,85} The enthalpy of fusion^{75,81,84,85} is 31.6–45.8 kJ mol⁻¹.

Sulfamethoxazole [C₁₀H₁₁N₃O₃S; 723-46-6; Benzenesulfonamide, 4-amino-N-(5-methyl-3-isoxazolyl)-]. The melting range according to handbooks is 167–173 °C. The chosen value^{10,83,86} is near 170 °C. The enthalpy of fusion is⁸⁴ 28.7 or^{10,86} 32.2 kJ mol⁻¹.

Sulfamethoxypridazine [C₁₁H₁₂N₄O₃S; 80-35-3; Benzenesulfonamide, 4-amino-N-(6-methoxy-3-pyridazinyl)-].

Handbook data for the melting point indicate 180–183 °C, and a value near the lower is probably accurate.^{10,81,83,87} The enthalpy of fusion^{10,81,83,87,88} lies in the range 29.0–32.6 kJ mol⁻¹.

Sulfanilamide [C₆H₈N₂O₂S; 63-74-1; Benzenesulfonamide, 4-amino-]. The handbook data indicate 164–167 °C as the melting range, and 165 °C was adopted.^{76,82} Since there is no experimental value for the enthalpy of fusion, it was estimated (next section).

Sulfapyridine [C₁₁H₁₁N₃O₂S; 144-83-2; Benzenesulfonamide, 4-amino-N-2-pyridinyl-]. The handbook melting range is 191–193 °C. The adopted value^{35,64} is close to 191 °C. The enthalpy of fusion is the mean of two measurements.^{32,81}

Sulfathiazole [C₉H₉N₃O₂S₂; 72-14-0; Benzenesulfonamide, 4-amino-N-2-thiazolyl-]. The melting range according to handbooks is 200–204 °C. A value close to the lower limit was adopted.^{23,75,76,84} The enthalpy of fusion lies in the range^{23,75,84} 24.1–28.9 kJ mol⁻¹.

Sulfisoxazole [C₁₁H₁₃N₃O₃S; 127-69-5; Benzenesulfonamide, 4-amino-N-(3,4-dimethyl-5-isoxazolyl)-]. Handbook data indicate 194–198 °C for the melting range. The adopted value was taken from experimental results.^{81,84} The enthalpy of fusion is the mean of two measurements.^{81,84}

Theophylline [C₇H₈N₄O₂; 58-55-9; 1H-Purine-2,6-dione, 3,7-dihydro-1,3-dimethyl-]. The melting range is 268–274 °C according to handbooks. The adopted value^{41,72} is the upper limit. There is one datum⁴¹ for the enthalpy of fusion.

Thiourea [CH₄N₂S; 62-56-6]. The handbook data indicate 175–182 °C as the melting range. An otherwise reliable compilation⁴⁰ states 172.4 °C. The adopted value was taken from a phase diagram measurement.⁴³ There is one datum⁴⁰ for the enthalpy of fusion.

Trimethoprim [C₁₄H₁₈N₄O₃; 738-70-5; 2,4-Pyrimidinediamine, 5-[(3,4,5-trimethoxyphenyl)methyl]-]. Handbook data for the melting point are 199–203 °C. The adopted value is close to the lower limit.^{10,83,86} There is one value for the enthalpy of fusion.¹⁰

Urea [CH₄N₂O; 57-13-6]. The handbook melting point is 132.6 °C, while a survey of phase diagram measurements gave a range of 130–134 °C, perhaps with some decomposition.⁸⁹ The enthalpy of fusion found experimentally^{30,90–93} lies in the range 13.0–15.5 kJ mol⁻¹.

It should be mentioned that no claim is made concerning the ultimate accuracy of the data in Table 1. The aim was to obtain reasonably accurate data for the purpose of calculating phase diagrams.

9. Estimation of Enthalpy of Fusion

For some compounds in Table 1, experimental enthalpies of fusion were unavailable and so they were estimated by one of several methods, described here.

For chemically simpler molecules, a group-contribution method⁹⁴ is useful. The enthalpy of fusion of aspirin was estimated by this method.

In Sec. 4, Eq. (1) relates the limiting liquidus slope in a phase diagram to the enthalpy of fusion of a pure component. Thus a phase diagram can be a source of experimental data for the enthalpy of fusion. In choosing phase diagram data for this purpose, attention was paid to the overall quality of the phase diagram data and to the possibility that the initial slope was obscured by deviations caused by large nonidealities of the liquid phase. The enthalpies of fusion of the following substances were found in this way (the reference indicates the source of the phase diagram data): succinimide,⁸⁰ nicotinic acid,^{95,96} sulfanilamide,⁹⁷ quinine⁹⁸ and chlormadinone acetate.⁵⁴

It is a commonly observed fact that the entropies of fusion of chemically and structurally similar organic compounds are also similar. This approximation was exploited in the estimation of the enthalpy of fusion of three substances. Thus, for isonicotinamide, the experimental entropy of fusion of the 3-isomer (nicotinamide) is 57.64 J mol⁻¹ K⁻¹. Using the relation $\Delta_{\text{fus}}H = T_{\text{fus}}\Delta_{\text{fus}}S$, one obtains (430.4)(57.64) = 24.8 kJ mol⁻¹. For 3-methoxybenzoic acid, the entropy of fusion of the 4-isomer⁴⁰ is 62.04 J mol⁻¹ K⁻¹, where the required datum is 23.8 kJ mol⁻¹. For etofylline, the available entropy of fusion⁹⁹ was that for 8-ethyltheophylline, 68.23 J mol⁻¹ K⁻¹, where the required datum is 29.6 kJ mol⁻¹.

The uncertainty in these estimated data is about ±20%. This is greater than experimental error in, for example, DSC measurements. The effect of this uncertainty in the calculation of phase diagrams (Figs. 1–60) is to add incrementally to the uncertainty in deduced excess Gibbs energy of the liquid and thermodynamic properties of intermediate compounds. The main features of the diagram are not affected. In the binary systems sulfanilamide-benzocaine, sulfanilamide-4-aminobenzoic acid and chlormadinone acetate-ethinyl estradiol, the enthalpy of fusion of one component was derived from the phase diagram under thermodynamic analysis. In these cases there is a slight circularity in the thermodynamic argument, which, however, had little practical effect.

10. Temperature Dependence of Enthalpy of Fusion

In the present work, phase diagrams are calculated on the assumption that the enthalpies of fusion of pure components are independent of temperature. This is equivalent to assuming that the heat capacities of solid and liquid are the same at all temperatures. This is, of course, not strictly true. The magnitude of the error in consequence of this assumption may be seen from a specific example. The heat capacities of liquid and solid benzocaine have been measured near the melting point.⁵⁰ At the melting point, the given data are⁵⁰

$$T_{\text{fus}} = 89.7 \text{ °C (362.9 K)}, \quad (2)$$

$$\Delta_{\text{fus}}H = 22\,300 \text{ J mol}^{-1}, \quad (3)$$

$$\Delta_{\text{fus}}S = 61.449 \text{ J mol}^{-1} \text{ K}^{-1}, \quad (4)$$

TABLE 2. The temperature dependence of the enthalpy and entropy of fusion of benzocaine^a

	$T_{\text{fus}}-50$	$T_{\text{fus}}-20$	T_{fus}	$T_{\text{fus}}+20$	$T_{\text{fus}}+50$
$\Delta_{\text{fus}}H, \text{ J mol}^{-1}$	19 832	21 315	22 300	23 293	24 774
$\Delta_{\text{fus}}S, \text{ J mol}^{-1} \text{ K}^{-1}$	54.135	58.661	61.449	64.113	67.837

^aSee Ref. 50.

and the heat capacity data are:
for the solid

$$C_p = 18.95 + 0.724T \quad \text{J mol}^{-1} \text{ K}^{-1} \quad (T \leq T_{\text{fus}}), \quad (5)$$

$$C_p = 134.4 + 0.406T \quad \text{J mol}^{-1} \text{ K}^{-1} \quad (T \geq T_{\text{fus}}), \quad (6)$$

for the liquid

$$C_p = 68.4 + 0.724T \quad \text{J mol}^{-1} \text{ K}^{-1} \quad (T \leq T_{\text{fus}}), \quad (7)$$

$$C_p = 183.8 + 0.906T \quad \text{J mol}^{-1} \text{ K}^{-1} \quad (T \geq T_{\text{fus}}), \quad (8)$$

where T is in Kelvin. In Eqs. (5)–(8) it has been assumed that the heat capacity curve of a phase beyond its normal range of existence is parallel to that of the other phase.⁵⁰ The enthalpy and entropy of fusion at different temperatures can be calculated from thermodynamic first principles, using the given data of Eqs. (2)–(8). The behavior is summarized in Table 2, which shows that both enthalpy and entropy of fusion vary with temperature in a well-behaved fashion. The practical consequence of assuming temperature independence will manifest itself as an incremental error in the derived excess Gibbs energy of the liquid and thermodynamic properties of intermediate compounds. The main features of the phase diagram will remain unaffected.

11. Thermodynamic Analysis and Presentation of Results

For each binary system, the source and identity of the data are indicated, together with any stated information on eutec-

tic, peritectic or transition points. If there are intermediate compounds, stoichiometry, enthalpy of fusion, melting points or other information are mentioned, according to sources. The reported phase diagram data points are included in the calculated phase diagram; metastable transitions, if any, are mentioned but do not appear on the diagram. The general aspect of the phase diagram is noted, along with an overall assessment of data quality (scatter, adherence to thermodynamic constraints, etc.). Preliminary calculations and assumptions made prior to optimization, if any, are stated. The results of the calculation, in addition to the phase diagram, are given as calculated eutectic and peritectic temperatures and compositions, or melting points of congruent compounds. Calculated thermodynamic data are also presented: these include the Gibbs energy of fusion and of formation (from the pure liquids) of any intermediate compounds, as well as the excess Gibbs energy of the liquid. These quantities are designated $\Delta_{\text{fus}}G^o$, $\Delta_f G^o$ and $G^E(l)$, respectively. When the given data are sparse or contradictory, the probable nature of the phase diagram is discussed in the light of general thermodynamic principles and behavior of similar systems. Finally, an estimate of the uncertainty in the calculated diagram is made, indicating the degree of confidence appropriate to the calculations in each case.

Where there are more than one eutectic in a system, they may be referred to as E_1 , E_2 , etc., in the discussion for individual systems; peritectics are indicated by P .

In the present article, no far-reaching claims are made concerning the ultimate correctness of the calculated phase dia-

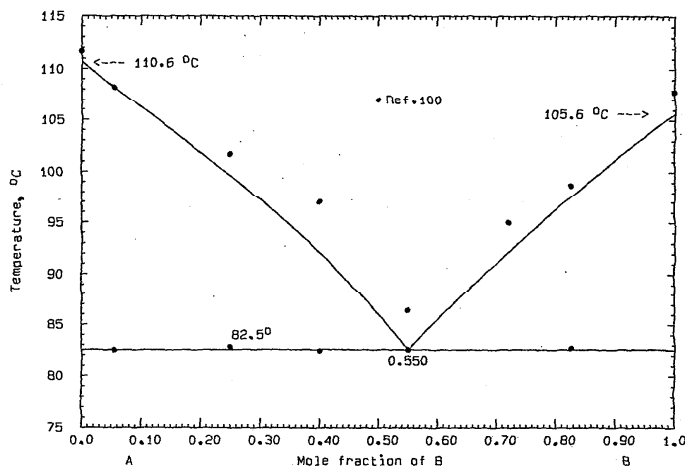


FIG. 1. The system phenazone (A)+phenylbutazone (B).

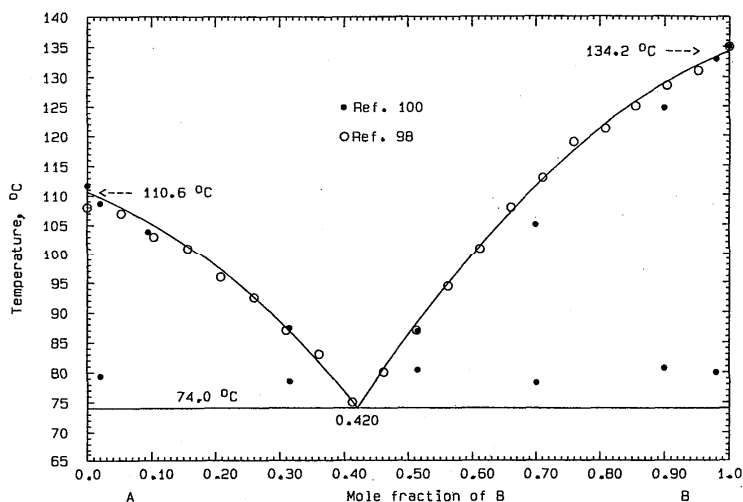


FIG. 2. The system phenazone (A)+phenacetin (B).

grams presented. This contribution represents the application of necessary thermodynamic constraints and consequent phase diagram interpretation which are pertinent for the analysis of solid-liquid equilibria generally.

12. Analysis of Phase Diagrams

12.1. Phenazone (A)+Phenylbutazone (B)

Data were obtained by DTA.¹⁰⁰ No eutectic information was stated. In the optimization, the eutectic data were preferentially weighted, as the liquidus data by themselves entailed a higher eutectic temperature than that observed. The phase diagram, Fig. 1, was calculated with the use of Eq. (9)

$$G^E(l) = x_A x_B (1278 - 810x_B) \text{ J mol}^{-1} \quad (9)$$

and the calculated eutectic is 82.5 °C, $x_B = 0.550$. An uncertainty of $\pm 4^\circ$ may be assigned to the diagram.

12.2. Phenazone (A)+Phenacetin (B)

Data were obtained by DTA¹⁰⁰ and the thaw-melt method.⁹⁸ The reported eutectic⁹⁸ is 75 °C, $x_B = 0.412$, but the eutectic data from DTA¹⁰⁰ lie higher than 75 °C. In a preliminary optimization, it was ascertained that the liquidus data are consistent with the observed⁹⁸ eutectic temperature and that the thaw-melt data⁹⁸ were of better quality. The phase diagram, Fig. 2, was calculated with the use of Eq. (10):

$$G^E(l) = x_A x_B (-6040 - 1207x_B) \text{ J mol}^{-1} \quad (10)$$

and the calculated eutectic is 74.0 °C, $x_B = 0.420$. An uncertainty of $\pm 2^\circ$ may be assigned to the calculated diagram.

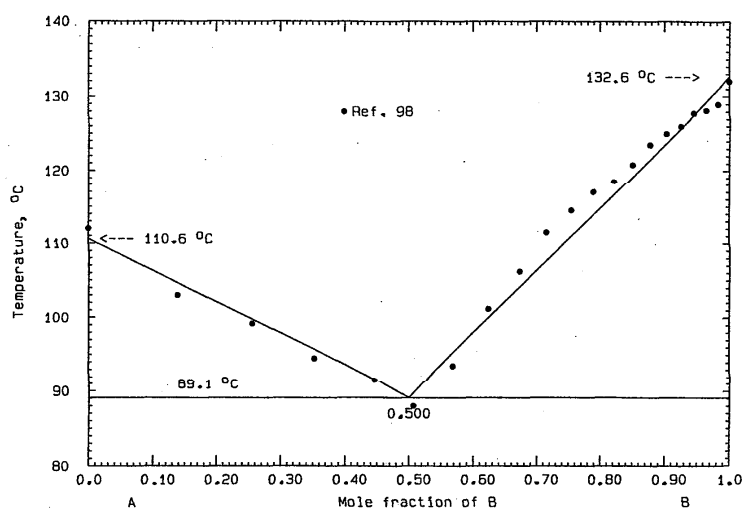


FIG. 3. The system phenazone (A)+urea (B).

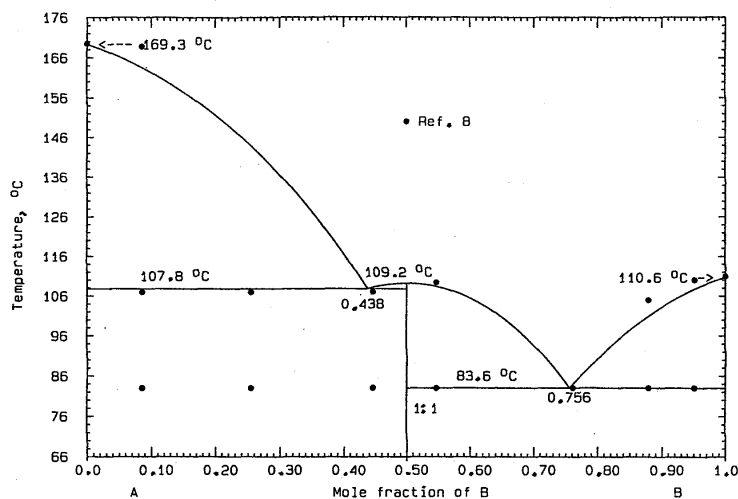


FIG. 4. The system paracetamol (A)+phenazone (B).

12.3. Phenazone (A)+Urea (B)

Data were obtained by the thaw-melt method.⁹⁸ The reported eutectic is 87 °C, $x_B=0.533$. All the liquidus data were optimized to give

$$G^E(l) = 2215x_Ax_B \text{ J mol}^{-1} \quad (11)$$

and the calculated phase diagram is given in Fig. 3. The calculated eutectic is 89.1 °C, $x_B=0.500$. An uncertainty of $\pm 2^\circ$ may be assigned to the calculated diagram.

12.4. Paracetamol (A)+Phenazone (B)

Data for the phase diagram were obtained by DTA using fused and physical mixtures.⁸ Only the data from fused mixtures are considered here and are shown in the calculated phase diagram. These data consisted of a number of thermo-

gram traces and a phase diagram with smoothed phase boundaries (no data points). The reported eutectic⁸ is 83 °C, $x_B=0.76$; the existence of a 1:1 congruently melting compound melting at 107 °C was considered possible. For the calculated phase diagram, the thermogram data were converted to liquidus, eutectic and peritectic data points and are shown on the phase diagram. An optimization was performed under the assumption of a eutectic temperature of 83 °C and the existence of a 1:1 compound. The phase diagram, Fig. 4, was calculated with the use of Eq. (12)

$$G^E(l) = x_Ax_B(-13122' - 4000x_B) \text{ J mol}^{-1}, \quad (12)$$

and the thermodynamic properties of the compound AB/2 are

$$\Delta_{\text{fus}}G^o = 23091 - 60.3926T \text{ J mol}^{-1}, \quad (13)$$

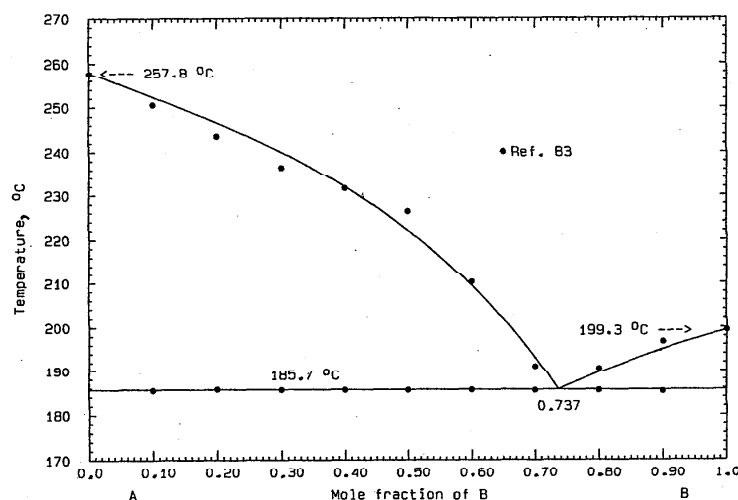


FIG. 5. The system sulfadiazine (A)+trimethoprim (B).

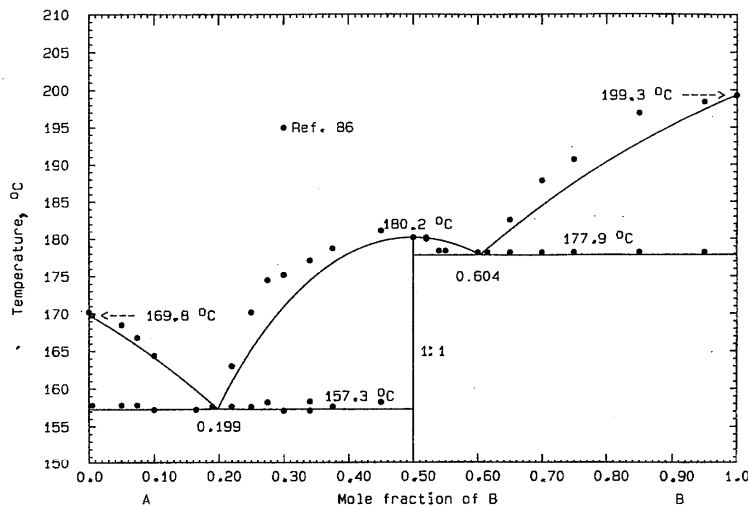


Fig. 6. The system sulfamethoxazole (A)+trimethoprim (B).

$$\Delta_f G^\circ = -26872 + 54.6314T \text{ J mol}^{-1}. \quad (14)$$

The calculated eutectics are 107.8 °C, $x_B=0.438$ and 83.6 °C, $x_B=0.756$. The 1:1 compound melts congruently at 109.2 °C. An uncertainty of $\pm 3^\circ$ may be assigned to the calculated diagram.

12.5. Sulfadiazine (A)+Trimethoprim (B)

Data were obtained by DSC⁸³ (the same data also appear in another publication¹⁰). The reported eutectic^{10,83} is 189.5 °C, $x_B=0.75$, although the plotted data^{10,83} show a eutectic temperature of 185.6 °C. The phase diagram, Fig. 5, was calculated with the use of Eq. (15)

$$G^E(l) = x_A x_B (-85 - 2546x_B) \text{ J mol}^{-1}, \quad (15)$$

and the calculated eutectic is 185.7 °C, $x_B=0.737$. An uncertainty of $\pm 2^\circ$ may be assigned to the calculated diagram.

12.6. Sulfamethoxazole (A)+Trimethoprim (B)

Phase diagram data were obtained by DSC.⁸⁶ The reported eutectics are 157.3 °C, $x_B=0.17$ and 177.9 °C, $x_B=0.61$. The 1:1 compound melted congruently at 180.2 °C. The compound was synthesized by mixing equimolar amounts of the components in water; the enthalpy of fusion of the dry compound was measured as 41.4 kJ mol⁻¹. The isolated compound was examined by photomicroscopy, x-ray diffraction and IR spectroscopy. The 1:1 compound¹⁰¹ is orthorhombic, $a=1.2055$ nm, $b=2.4476$ nm, $c=1.7423$ nm, space group Pbca, $Z=8$. All liquidus data were optimized, with the result

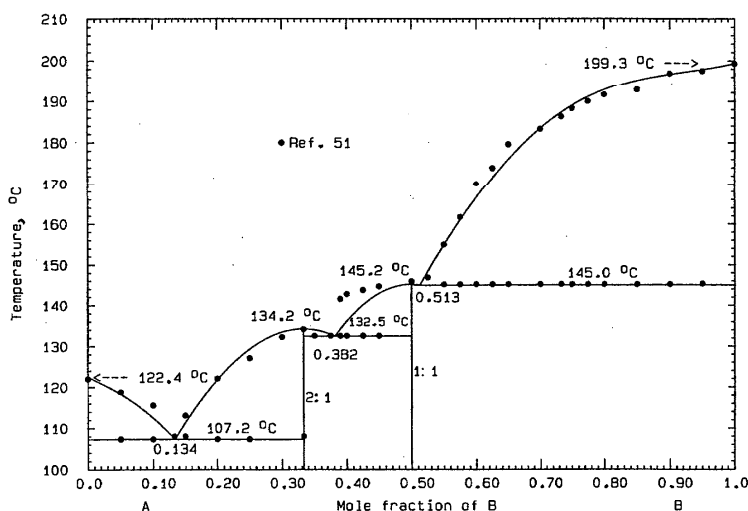


Fig. 7. The system benzoic acid (A)+trimethoprim (B).

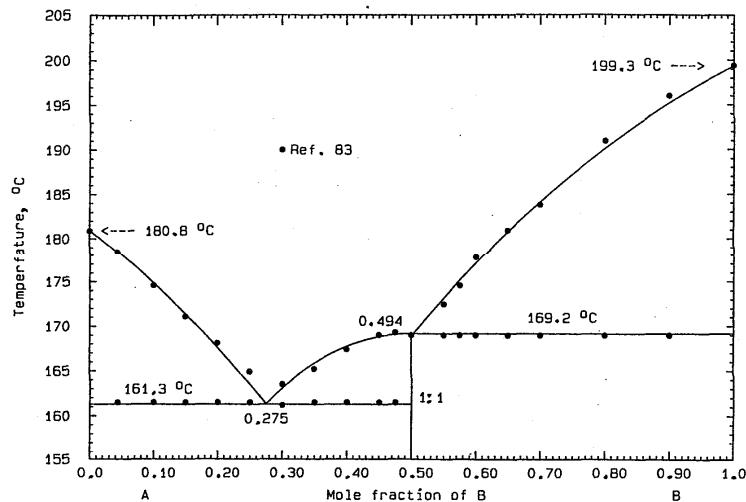


FIG. 8. The system sulfamethoxyypyridazine (A)+trimethoprim (B).

$$G^E(l) = x_A x_B (-2800 + 450x_B) \text{ J mol}^{-1} \quad (16)$$

for the liquid, and for the compound AB/2

$$\Delta_{\text{fus}}G^\circ = 21\,124 - 46.5950T \text{ J mol}^{-1}, \quad (17)$$

$$\Delta_f G^\circ = -21\,768 + 40.8322T \text{ J mol}^{-1}. \quad (18)$$

The calculated eutectics are 157.3 °C, $x_B = 0.199$ and 177.9 °C, $x_B = 0.604$. The compound melts at 180.2 °C; the calculated phase diagram is shown in Fig. 6. Some of the experimental liquidus data lie too high for thermodynamic consistency. An uncertainty of $\pm 1^\circ$ may be assigned to the calculated diagram.

12.7. Benzoic Acid (A)+Trimethoprim (B)

Phase diagram data were obtained by DSC.⁵¹ The reported eutectics are $E_1 = 106.8^\circ\text{C}$, $x_B = 0.14$; $E_2 = 132.5^\circ\text{C}$, $x_B = 0.37$; $E_3 = 145.0^\circ\text{C}$, $x_B = 0.52$. There are two intermediate compounds, 2:1 and 1:1 melting congruently at 134.2 and 145.9 °C, respectively. The 1:1 compound was prepared by mixing stoichiometric amounts of components in water or methanol or ethyl acetate. The 2:1 compound was also synthesized in the same way in water or diethyleneglycol solution. The 2:1 compound also has a metastable melting point of 126.5 °C. The enthalpies of fusion of the compounds were measured as 52.3 and 56.1 kJ mol⁻¹, respectively. X-ray and IR spectra were obtained for both compounds. The 1:1 compound is monoclinic, $a = 1.1295$ nm, $b = 2.8266$ nm, $c = 0.6543$ nm, $\beta = 100.97^\circ$, space group $P2_1/N$, $Z = 4$. The stable form of the 2:1 compound is triclinic, $a = 1.4595$ nm, $b = 1.0195$ nm, $c = 0.9455$ nm, $\alpha = 89.67^\circ$, $\beta = 97.37^\circ$, $\gamma = 104.6^\circ$, space group $P1$ or P_T , $Z = 2$. A thermal event, observed at 120.2 °C, was possibly a metastable eutectic between the 2:1 compound and trimethoprim.⁵¹

All liquidus data were optimized, with the result

$$G^E(l) = x_A x_B (-1800 - 14\,527x_B + 23\,746x_B^2) \text{ J mol}^{-1} \quad (19)$$

for the liquid. For the compound AB/2,

$$\Delta_{\text{fus}}G^\circ = 15\,422 - 36.8663T \text{ J mol}^{-1}, \quad (20)$$

$$\Delta_f G^\circ = -20\,254 + 31.1035T \text{ J mol}^{-1}, \quad (21)$$

and for A₂B/3

$$\Delta_{\text{fus}}G^\circ = 18\,450 - 45.2920T \text{ J mol}^{-1}, \quad (22)$$

$$\Delta_f G^\circ = -22\,940 + 40.0000T \text{ J mol}^{-1}. \quad (23)$$

The calculated eutectics (Fig. 7) are $E_1 = 107.2^\circ\text{C}$, $x_B = 0.134$; $E_2 = 132.5^\circ\text{C}$, $x_B = 0.382$; $E_3 = 145.0^\circ\text{C}$, $x_B = 0.513$. The calculated melting points of compounds are 134.2 °C and 145.2 °C. Most of the experimental liquidus data are shown to be consistent except for a few in the middle range. An uncertainty of $\pm 1^\circ$ may be assigned to the calculated diagram.

12.8. Sulfamethoxyypyridazine (A) + Trimethoprim (B)

Data were obtained by DSC⁸³ (the same data also appear in another publication¹⁰). The reported eutectics are 162.0 °C, $x_B = 0.29$ and 168.8 °C, $x_B = 0.51$. A metastable eutectic 148.4 °C was observed. The 1:1 compound melts congruently at 169.5 °C, and its enthalpy of fusion is 72.3 kJ mol⁻¹. It was synthesized¹⁰ from equimolar mixtures in 95% ethanol, methanol or water. X-ray and IR spectra were also taken.¹⁰ All liquidus data were optimized, and the experimental eutectic temperatures were weighted preferentially. For the liquid, the result is

$$G^E(l) = -2555x_A x_B \text{ J mol}^{-1} \quad (24)$$

and for the compound AB/2

$$\Delta_{\text{fus}}G^\circ = 30\,234 - 68.3507T \text{ J mol}^{-1}, \quad (25)$$

$$\Delta_f G^\circ = -30\,873 + 62.5896T \text{ J mol}^{-1}. \quad (26)$$

The calculated phase diagram is shown in Fig. 8. The calcu-

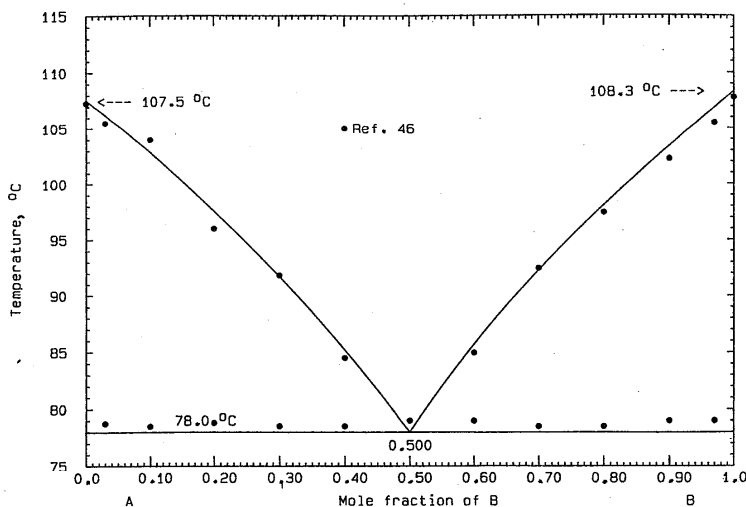


FIG. 9. The system aminophenazone (A)+4-aminophenazone.

lated data are $E=161.3^{\circ}\text{C}$, $x_B=0.275$ and $P=169.2^{\circ}\text{C}$, $x_B=0.494$. Within experimental uncertainty, the compound could be either congruently or incongruently melting. The experimental liquidus data are well reproduced. An uncertainty of $\pm 1^{\circ}$ may be assigned to the calculated diagram.

12.9. Aminophenazone (A)+4-Aminophenazone (B)

Phase diagram data were obtained by DSC, DTA and the microthermal methods.⁴⁶ The reported eutectic is 79°C , $x_B=0.50$. The eutectic mixture was examined by photomicroscopy. The liquidus data from the three methods are in very good agreement, and not all are shown on the phase diagram. From the optimization, the result is

$$G^E(l) = x_A x_B (-482 + 657 x_B) \text{ J mol}^{-1}, \quad (27)$$

and the calculated phase diagram appears in Fig. 9. The li-

quidus data are consistent with a slightly lower calculated eutectic, 78.0°C , $x_B=0.500$. An uncertainty of $\pm 2^{\circ}$ may be assigned to the phase diagram.

12.10. Aminophenazone (A)+Phenacetin (B)

Data were obtained by DTA¹⁰⁰ and no eutectic data were stated. All liquidus data were optimized, with preferential weighting for the observed eutectic temperature. For the liquidus,

$$G^E(l) = x_A x_B (-5112 + 5066 x_B) \text{ J mol}^{-1} \quad (28)$$

and the calculated phase diagram is shown in Fig. 10. The calculated eutectic is 82.0°C , $x_B=0.320$. An uncertainty of $\pm 3^{\circ}$ may be assigned to the calculated diagram.

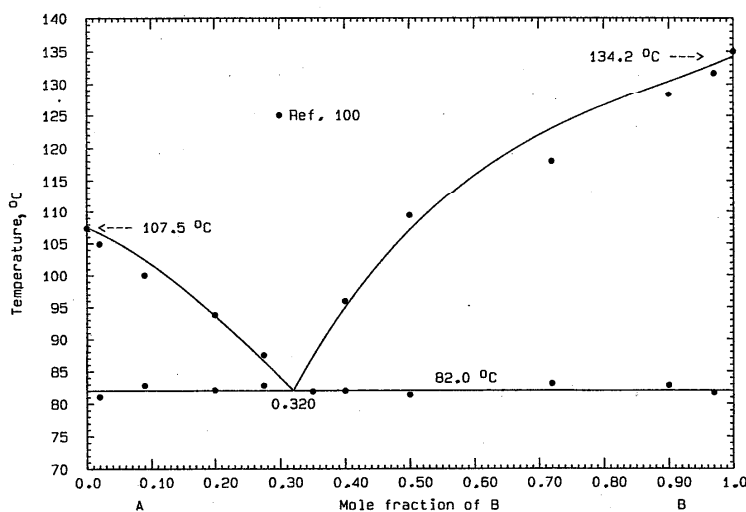


FIG. 10. The system aminophenazone (A)+phenacetin (B).

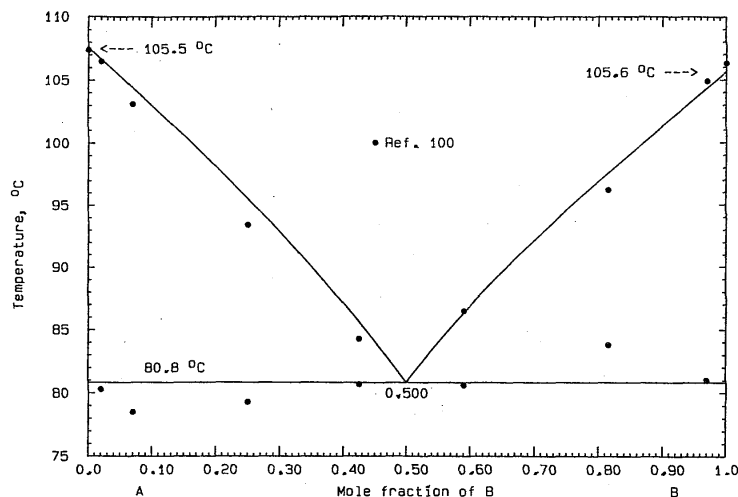


FIG. 11. The system aminophenazone (A)+phenylbutazone (B).

12.11. Aminophenazone (A)+Phenylbutazone (B)

Data were obtained by DTA¹⁰⁰ and no eutectic data were stated. There is scatter in the observed eutectic arrests. All the liquidus data were optimized, with preferential weighting of a eutectic temperature given by data near the eutectic composition. For the liquid,

$$G^E(l) = x_A x_B (415 + 489x_B) \text{ J mol}^{-1} \quad (29)$$

and the calculated phase diagram is shown in Fig. 11. The calculated eutectic is 80.8 °C, $x_B = 0.500$. An uncertainty of $\pm 4^\circ$ may be assigned to the calculated diagram.

12.12. Aminophenazone (A)+Phenazone (B)

Liquidus data were obtained by DSC⁴⁶, DTA^{46,100} and hot-stage microscopy.⁴⁶ Data obtained by the three methods were in good agreement. The observed eutectic⁴⁶ is 81.2 °C, x_B

= 0.48. The eutectic mixture was examined by photomicroscopy.⁴⁶ In the optimization, all liquidus data were weighted equally, and the result is

$$G^E(l) = x_A x_B (-168 + 950x_B) \text{ J mol}^{-1}. \quad (30)$$

The calculated phase diagram is shown in Fig. 12, with a calculated eutectic of 81.6 °C, $x_B = 0.463$. It is apparent that the older data⁴⁶ are of better quality than the other. An uncertainty of $\pm 1^\circ$ may be assigned to the calculated diagram.

12.13. Thiourea (A) and Aminophenazone (B)

Data were obtained by DSC and light transmission⁴³ and are in good agreement. The reported eutectic is 92 °C, $x_B = 0.73$ and peritectic 138 °C, $x_B = 0.27$. From x-ray diffraction spectra, the stoichiometry of the compound was found to be 3:1. Optimization of liquidus data resulted in Eq. (31)

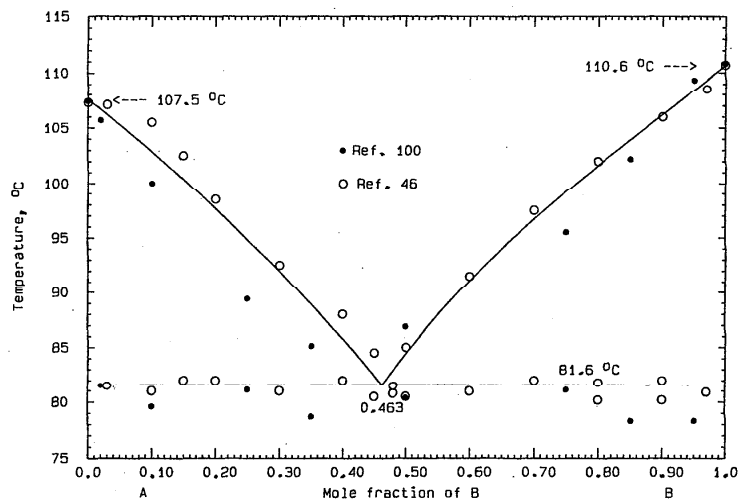


FIG. 12. The system aminophenazone (A)+phenazone (B).

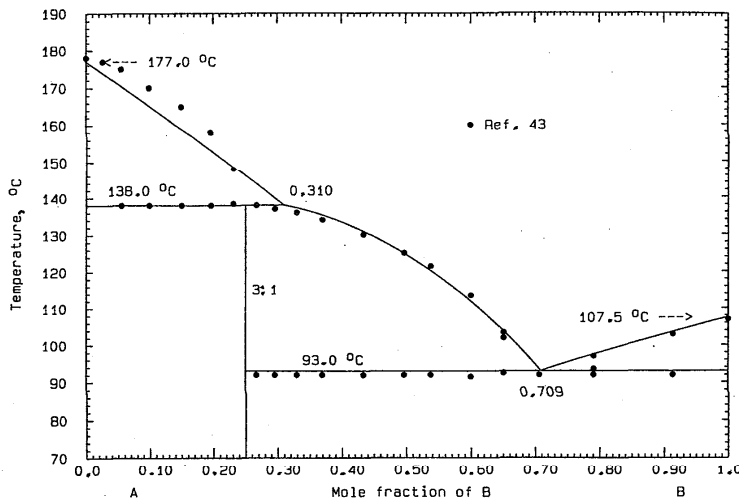


FIG. 13. The system thiourea (A)+aminophenazone (B).

$$G^E(l) = x_A x_B (134 - 150x_B) \text{ J mol}^{-1} \quad (31)$$

For the liquid, and for the compound $A_3B/4$

$$\Delta_{\text{fus}}G^\circ = 12\,198 - 29.5956T, \quad (32)$$

$$\Delta_1 G^\circ = -12\,180 + 24.9217T. \quad (33)$$

The calculated diagram appears in Fig. 13 and the calculated invariant points are

$$E = 93.0^\circ\text{C}, \quad x_B = 0.310.$$

The experimental data are well reproduced and an uncertainty of $\pm 1^\circ$ may be assigned to the calculated diagram.

12.14. Urea (A)+Aminophenazone (B)

Data were obtained by DSC and light transmission⁴³ and are in good agreement. The reported eutectics are E_1

$= 125^\circ\text{C}$, $x_B = 0.21$ and $E_2 = 97.5^\circ\text{C}$, $x_B = 0.80$. A 3:1 compound melts congruently at 125°C . The limiting liquidus slope at the left hand side (LHS) definitely suggests some solid solubility there, although none was mentioned by the investigators.⁴³ Some liquidus data at $x_B > 0.5$ proved to be grossly inaccurate. The E_1 and compound melting temperatures were evidently very close. In these circumstances, it was decided to construct a phase diagram using Eq. (34)

$$G^E(l) = 0, \quad (34)$$

and a solid solution with properties such that the calculated E_1 temperature would be near the observed datum. The thermodynamic properties of the compounds could not be obtained from optimization, and hence reasonable values were assigned for $A_3B/4$:

$$\Delta_{\text{fus}}G^\circ = 28\,000 - 70.0000T \text{ J mol}^{-1}, \quad (35)$$

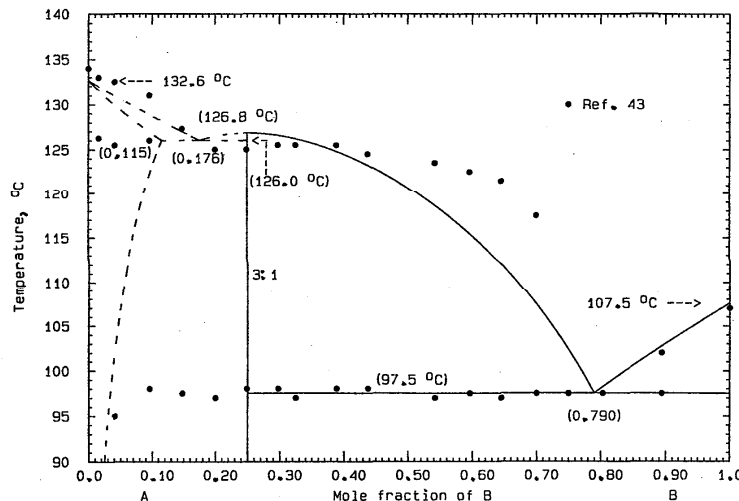


FIG. 14. The system urea (A)+aminophenazone (B). Part of the diagram is conjectural.

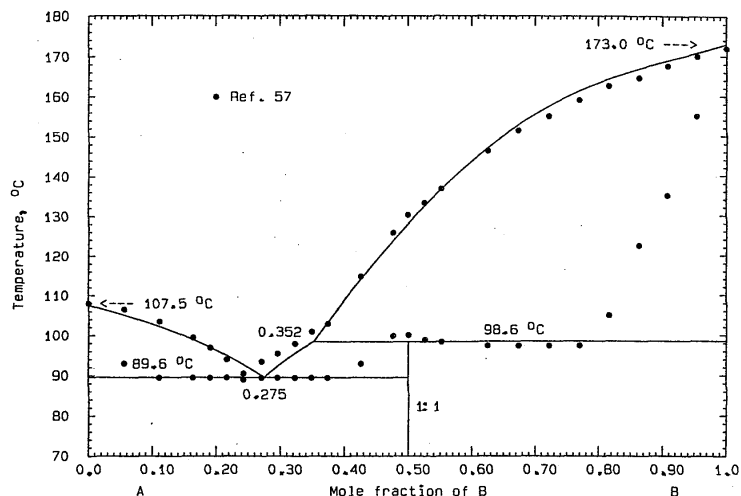


FIG. 15. The system aminophenazone (A)+allobarbital (B).

$$\Delta_f G^\circ = -28\,000 + 65.3248T \quad \text{J mol}^{-1}. \quad (36)$$

The solid solution based on urea was represented by a Henrian activity coefficient independent of temperature given by

$$RT \ln \gamma_B = 50 \quad \text{J mol}^{-1}. \quad (37)$$

The calculated phase diagram is given in Fig. 14, and the calculated eutectics are $E_1 = 126.8^\circ\text{C}$, $x_B = 0.176$; $E_2 = 97.5^\circ\text{C}$, $x_B = 0.790$. The compound melts at 126.8°C and the solid solution extends to 11.5 mole % at the eutectic temperature. The entire phase diagram is suggestive only.

12.15. Aminophenazone (A)+Allobarbital (B)

Data were obtained by the thaw-melt method from physical and fused mixtures⁵⁷ (only data from fused mixtures are shown in the phase diagram). No invariant points were stated, but the presence of an incongruently melting 1:1 com-

pound was postulated. The compound was synthesized from stoichiometric quantities of components in water solution. There was a metastable eutectic⁵⁷ at about 80°C . All liquidus data were used in the optimization, with preferential weighting for observed eutectic and peritectic temperatures. For the liquid, the result was

$$G^E(l) = x_A x_B (-4227 - 5722x_B + 8323x_B^2) \quad \text{J mol}^{-1}, \quad (38)$$

and for the compound AB/2

$$\Delta_{\text{fus}} G^\circ = 16\,563 - 43.7452T \quad \text{J mol}^{-1}, \quad (39)$$

$$\Delta_f G^\circ = -17\,815 + 37.9840T \quad \text{J mol}^{-1}. \quad (40)$$

The calculated phase diagram is shown in Fig. 15. The cal-

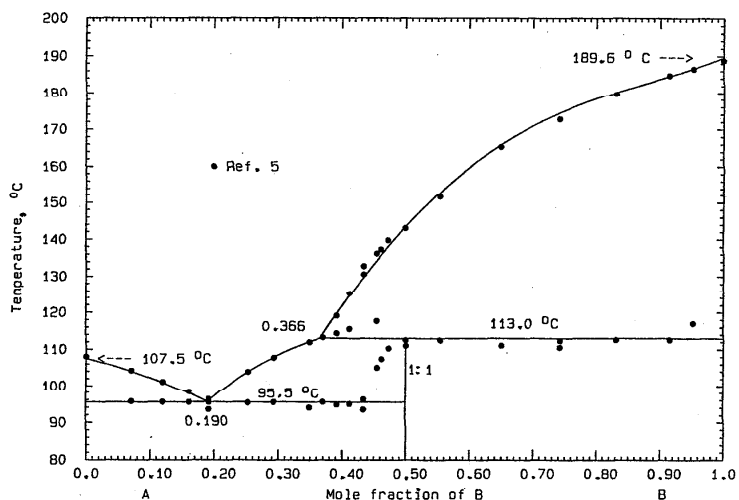


FIG. 16. The system aminophenazone (A)+barbital (B).

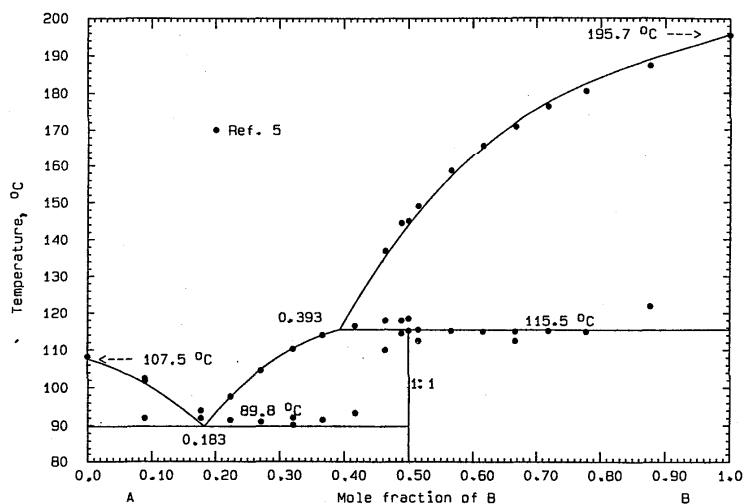


Fig. 17. The system aminophenazone (A)+sulfisoxazole (B).

culated invariant points are $E=89.6^{\circ}\text{C}$, $x_B=0.275$ and $P=98.6^{\circ}\text{C}$, $x_B=0.352$. An uncertainty of $\pm 2^{\circ}$ may be assigned to the calculated diagram.

12.16. Aminophenazone (A)+Barbital (B)

Data were obtained by the thaw-melt method with both fused and solvent-evaporated mixtures.⁵ The results from the two series are in good agreement. No invariant points were stated, but a metastable eutectic at about 88°C was observed. A 1:1 compound, which was synthesized from equimolar amounts of components in water solution, melted incongruently. All liquidus data were optimized, with the result

$$G^E(l) = x_A x_B (-4583 + 636x_B + 4905x_B^2) \quad \text{J mol}^{-1} \quad (41)$$

for the liquid and

$$\Delta_{\text{fus}}G^{\circ} = 25170 - 64.6175T \quad \text{J mol}^{-1}, \quad (42)$$

$$\Delta_{\text{f}}G^{\circ} = -25930 + 58.8563T \quad \text{J mol}^{-1} \quad (43)$$

for the compound AB/2. The calculated phase diagram appears in Fig. 16, and the calculated invariant points are $E=95.5^{\circ}\text{C}$, $x_B=0.190$ and $P=113.0^{\circ}\text{C}$, $x_B=0.366$. The liquidus data are well reproduced. An uncertainty of $\pm 2^{\circ}$ may be assigned to the calculated diagram.

12.17. Aminophenazone (A)+Sulfisoxazole (B)

Data were obtained by the thaw-melt method on both used and solvent-evaporated mixtures.⁵ The data from the two series are in good agreement. No invariant points were stated by the authors, but a metastable eutectic at about 82°C was mentioned. The 1:1 compound was synthesized from equimolar amounts of components in water solution; DTA

on this compound indicated an incongruent melting point of 115.6°C . An optimization was performed on all the liquidus data, with the results

$$G^E(l) = x_A x_B (-13908 + 10207x_B) \quad \text{J mol}^{-1} \quad (44)$$

for the liquid and

$$\Delta_{\text{fus}}G^{\circ} = 32267 - 82.5133T \quad \text{J mol}^{-1}, \quad (45)$$

$$\Delta_{\text{f}}G^{\circ} = -34468 + 76.7521T \quad \text{J mol}^{-1} \quad (46)$$

for the compound AB/2. The calculated phase diagram is shown in Fig. 17 and the calculated eutectic is 89.8°C , $x_B=0.183$; peritectic 115.5°C , $x_B=0.393$. The experimental liquidus data are well reproduced and an uncertainty of $\pm 2^{\circ}$ may be assigned to the calculated diagram.

12.18. 3-Methoxybenzoic Acid (A)+Etofylline (B)

Data were obtained by the thaw-melt method⁵⁷ with both physical and fused mixtures (only the results for fused mixtures are shown on the diagram). No invariant points were stated, but a metastable eutectic at about 85°C was observed. A 1:1 compound melts incongruently. All liquidus data were optimized, with the results

$$G^E(l) = x_A x_B (-5497 + 4288x_B) \quad \text{J mol}^{-1}, \quad (47)$$

for the liquid and

$$\Delta_{\text{fus}}G^{\circ} = 22526 - 60.0322T \quad \text{J mol}^{-1}, \quad (48)$$

$$\Delta_{\text{f}}G^{\circ} = -23364 + 54.2694T \quad \text{J mol}^{-1} \quad (49)$$

for the compound AB/2. The calculated phase diagram is shown in Fig. 18, and the calculated data are $E=89.0^{\circ}\text{C}$, $x_B=0.249$ and $P=98.0^{\circ}\text{C}$, $x_B=0.358$. The experimental liquidus data are well reproduced (the experimental melting point of 3-methoxybenzoic acid is 4° too low) and an uncertainty of $\pm 1^{\circ}$ may be assigned to the calculated diagram.

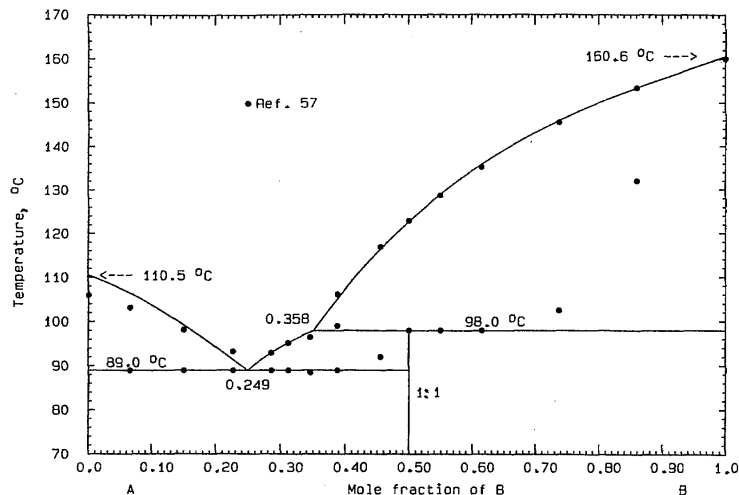


FIG. 18. The system 3-methoxybenzoic acid (A)+etofylline (B).

12.19. Benzoic Acid (A)+Etofylline (B)

Data were obtained by the thaw-melt method⁵⁷ on physical, fused and solvent-evaporated mixtures (only results from fused and solvent-evaporated mixtures are shown on the phase diagram). A metastable eutectic at about 94 °C was observed, but no other invariant point information was given. A 1:1 compound melts incongruently. All liquidus data were optimized. For the liquid,

$$G^E(l) = x_A x_B (-189 + 742 x_B) \text{ J mol}^{-1}, \quad (50)$$

and for the compound AB/2

$$\Delta_{\text{fus}} G^o = 18\,581 - 48.5705T \text{ J mol}^{-1}, \quad (51)$$

$$\Delta_{\text{fus}} G^o = -18\,961 + 42.8093T \text{ J mol}^{-1} \quad (52)$$

were derived. The calculated phase diagram appears in Fig. 19 and calculated invariant points are $E=98.5^\circ\text{C}$, x_B

$=0.257$; $P=106.4^\circ\text{C}$, $x_B=0.367$. An uncertainty of $\pm 2^\circ$ may be assigned to the calculated phase diagram.

12.20. Aminophenazone (A)+Etofylline (B)

Data were obtained by the thaw-melt method⁵⁷ on both physical and fused mixtures (only fused mixture data are shown on the phase diagram). A metastable eutectic of 101 °C was reported, but no other information was offered. The liquidus data could be fit very well by an expression

$$G^E(l) = x_A x_B (2934 - 1029 x_B + 2729 x_B^2) \text{ J mol}^{-1} \quad (53)$$

and the calculated phase diagram is shown in Fig. 20. The liquidus data entail a eutectic 101.8°C , $x_B=0.142$; this temperature is significantly above the experimental datum

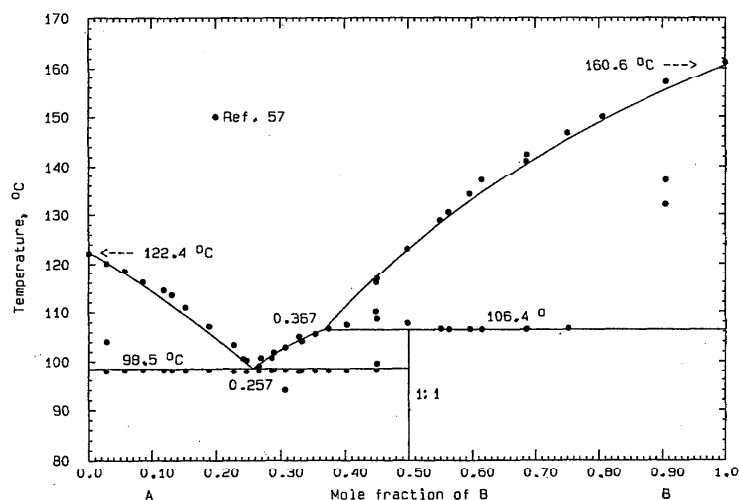


FIG. 19. The system benzoic acid (A)+etofylline (B).

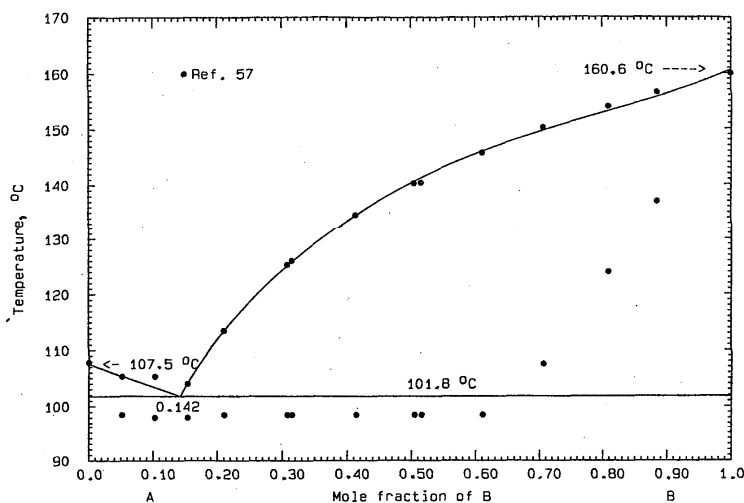


FIG. 20. The system aminophenazone (A)+etofylline (B).

(98 °C) but the phase boundaries shown in Fig. 20 are thermodynamically self-consistent. An uncertainty of $\pm 2^\circ$ may be assigned to the calculated diagram.

12.21. 4-Nitroaniline (A)+Etofylline (B)

Data were obtained with the thaw-melt method⁵⁷ on physical and fused mixtures (only data from fused mixtures are shown in the phase diagram). No invariant points were reported, but a metastable eutectic at 111 °C was observed, as well as the existence of an incongruently melting 1:1 compound. In a preliminary calculation, it was ascertained that the liquidus data entail eutectic and peritectic temperatures consistently higher than those observed. For constructing the phase diagram, therefore, these temperatures were preferen-

tially weighted and thermodynamic properties of the compound were assigned to reproduce the experimental data as closely as possible. For the liquid,

$$G^E(l) = x_A x_B (-800 + 570 x_B) \text{ J mol}^{-1} \quad (54)$$

and for the compound AB/2

$$\Delta_{\text{fus}} G^\circ = 10\,121 - 25.7628T \text{ J mol}^{-1}, \quad (55)$$

$$\Delta_f G^\circ = -10\,250 + 20.0000T \text{ J mol}^{-1}. \quad (56)$$

The calculated phase diagram is shown in Fig. 21 and the calculated invariant points are $E = 115.0^\circ\text{C}$, $x_B = 0.372$ and $P = 118.0^\circ\text{C}$, $x_B = 0.422$. An uncertainty of $\pm 2^\circ$ may be assigned to the calculated diagram.

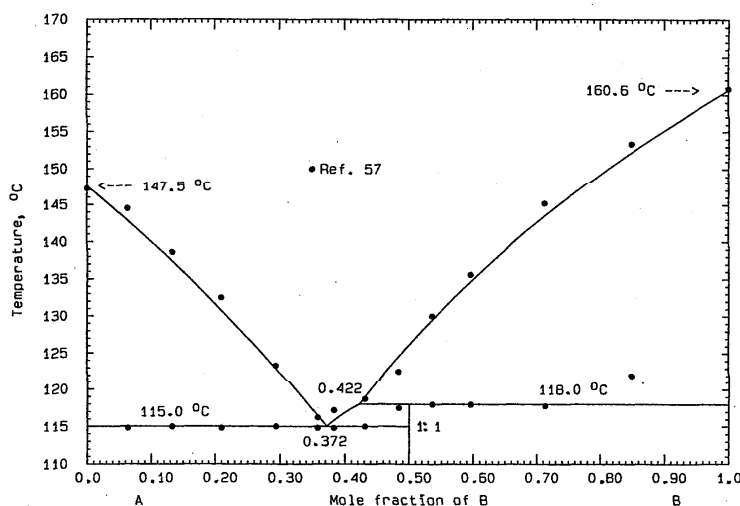


FIG. 21. The system 4-nitroaniline (A)+etofylline (B).

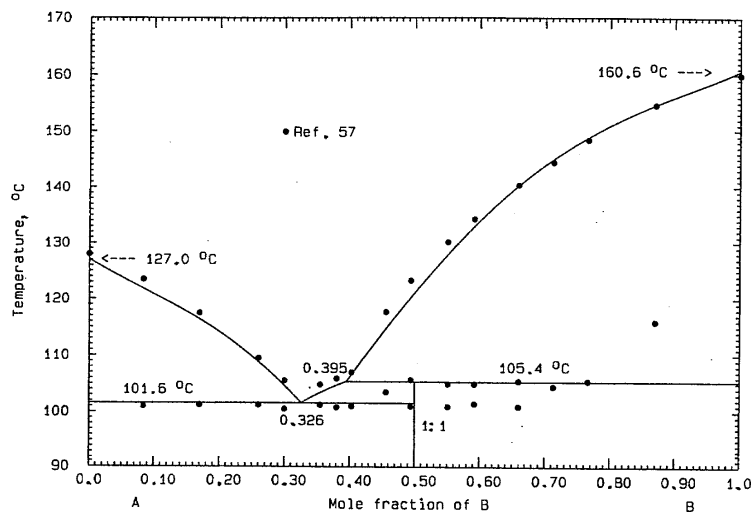


FIG. 22. The system benzidine (A)+etofylline (B).

12.22. Benzidine (A)+Etofylline (B)

Data were obtained by the thaw-melt method⁵⁷ on physical and fused mixtures (only the fused mixture data are shown on the phase diagram). A metastable eutectic at about 98 °C and an incongruently melting 1:1 compound were reported, but no other information. All liquidus data were optimized with the results

$$G^E(l) = x_A x_B (100 - 7981x_B + 8302x_B^2) \text{ J mol}^{-1}, \quad (57)$$

for the liquid and

$$\Delta_{\text{fus}}G^o = 18932 - 49.7207T \text{ J mol}^{-1}, \quad (58)$$

$$\Delta_f G^o = -19386 + 43.9596T \text{ J mol}^{-1} \quad (59)$$

for the compound AB/2. The calculated phase diagram is shown in Fig. 22, with $E = 101.6^\circ\text{C}$, $x_B = 0.326$ and P

$= 105.4^\circ\text{C}$, $x_B = 0.395$. An uncertainty of $\pm 2^\circ$ may be assigned to the calculated diagram.

12.23. Hydroquinone (A)+Etofylline (B)

Data were obtained by the thaw-melt method⁵⁷ on both physical and fused mixtures (only data from fused mixtures are shown in the phase diagram). Although no invariant point data were stated, metastable eutectics at about 121 °C and 113 °C and the presence of a congruently melting 3:2 compound were mentioned. The liquidus data from physical mixtures coincided with those from fused mixtures (other temperature arrests did not). The liquidus data themselves entailed eutectic temperatures higher than those observed, and so in the optimization greater weight was given to these temperatures. For the liquid,

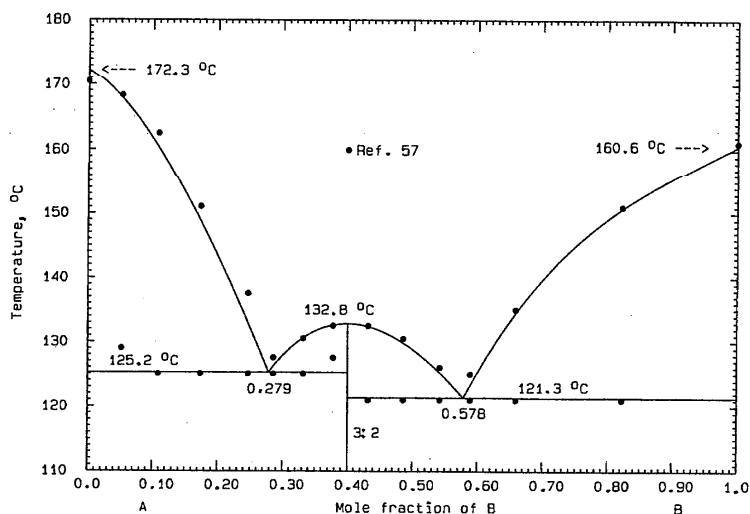


FIG. 23. The system hydroquinone (A)+etofylline (B).

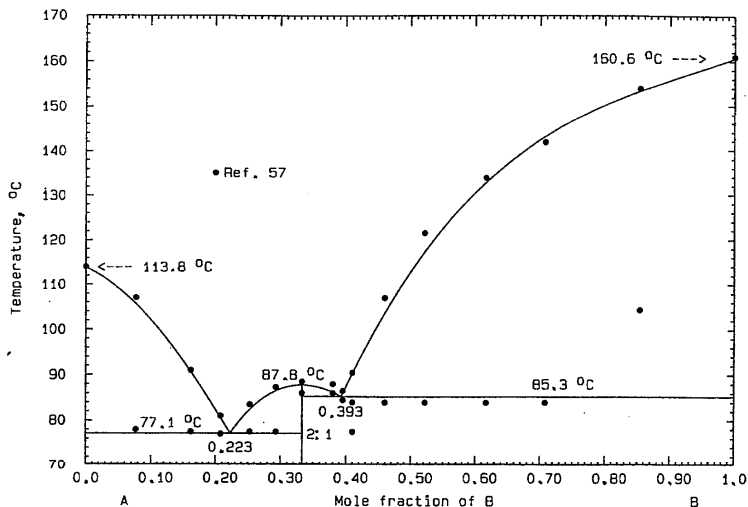


FIG. 24. The system 4-nitrophenol (A)+etofylline (B).

$$G^E(l) = x_A x_B (-18000 + 11248x_B) \text{ J mol}^{-1}, \quad (60)$$

and for the compound $A_3B_2/5$

$$\Delta_{\text{fus}}G^\circ = 20635 - 50.8257T \text{ J mol}^{-1}, \quad (61)$$

$$\Delta_f G^\circ = -23875 + 45.2319T \text{ J mol}^{-1}. \quad (62)$$

The calculated phase diagram is shown in Fig. 23 and calculated invariant points are $E_1 = 125.2^\circ\text{C}$, $x_B = 0.279$; $E_2 = 121.3^\circ\text{C}$, $x_B = 0.578$. The compound melts at 132.8°C . An uncertainty of $\pm 2^\circ$ may be assigned to the calculated diagram.

12.24. 4-Nitrophenol (A)+Etofylline (B)

Data were obtained by the thaw-melt method⁵⁷ on physical and fused mixtures (only data from fused mixtures are shown

in the diagram). Although no invariant point data were stated, a metastable eutectic at about 57°C and the existence of a 2:1 congruently melting compound were noted. All liquidus data were optimized, and the calculated phase diagram (Fig. 24) was constructed with the quantities

$$G^E(l) = x_A x_B (-15000 + 10318x_B) \text{ J mol}^{-1}, \quad (63)$$

and

$$\Delta_{\text{fus}}G^\circ = 10064 - 27.8834T \text{ J mol}^{-1}, \quad (64)$$

$$\Delta_f G^\circ = -12633 + 22.5949T \text{ J mol}^{-1} \quad (65)$$

for the compound $A_2B/3$. Other calculated data are: $E_1 = 77.1^\circ\text{C}$, $x_B = 0.223$ and $E_2 = 85.3^\circ\text{C}$, $x_B = 0.393$. An uncertainty of $\pm 4^\circ$ may be assigned to the calculated diagram.

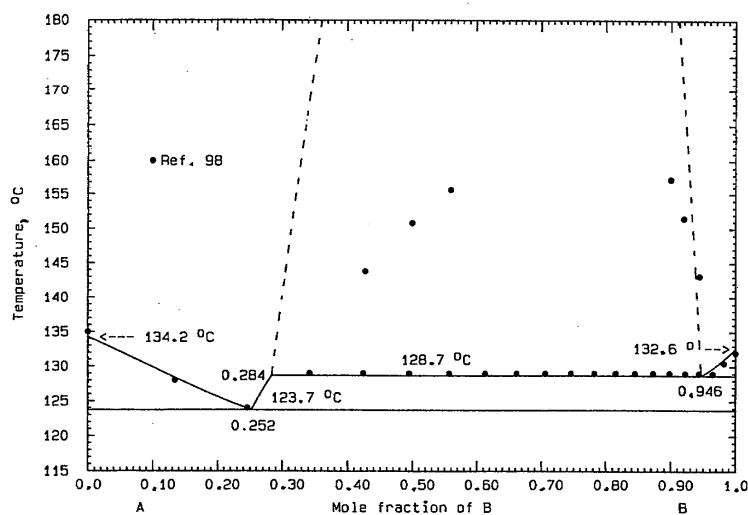


FIG. 25. The system phenacetin (A)+urea (B). The calculated immiscibility envelope is conjectural.

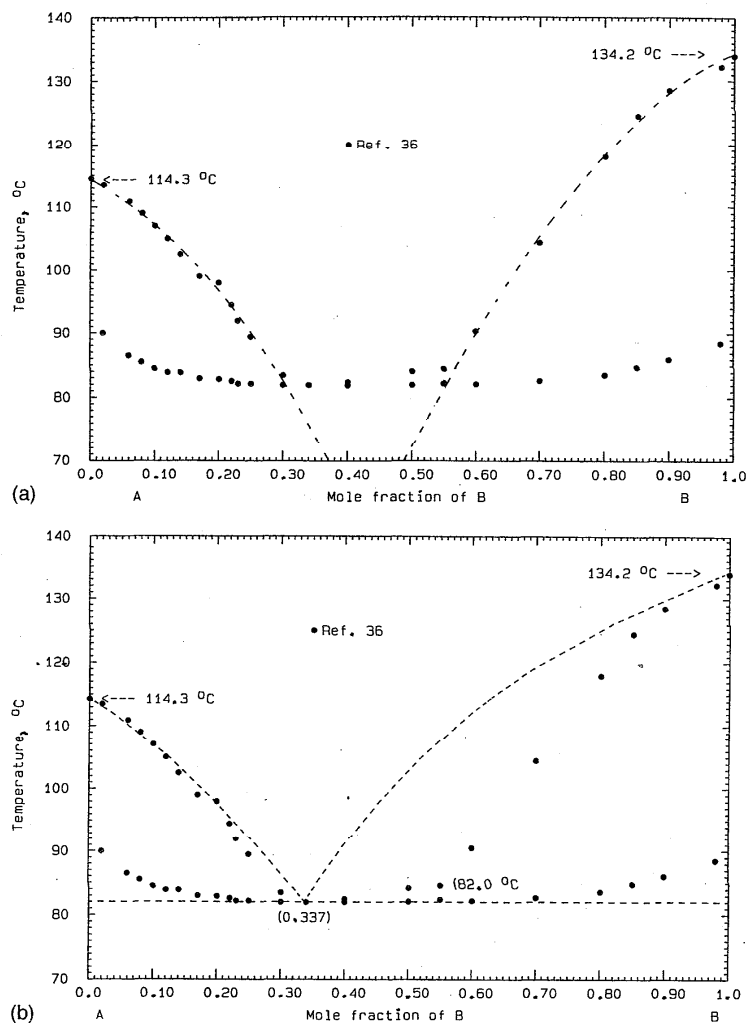


FIG. 26. (a) The system acetanilide (A)+phenacetin (B). A possible interpretation of the data. (b) The system acetanilide (A)+phenacetin (B). Another possible interpretation of the data.

12.25. Phenacetin (A)+Urea (B)

Data were obtained by the thaw-melt method.⁹⁸ Liquidus and monotectic data were tabulated, but data defining the liquid miscibility gap were available only as points on a phase diagram. The eutectic was reported to be 129.0 °C, $x_B = 0.305$, and the liquid miscibility gap lay in the range $0.342 < x_B < 0.963$. The consolute point, read off the phase diagram, was ~ 164 °C, $x_B \sim 0.78$. It was found that a consolute temperature as low as that experimentally suggested⁹⁸ was inconsistent with the remaining (better established) diagram. The experimental monotectic temperature (128.7 °C) was well reproduced by the quantity

$$G^E(l) = x_A x_B (4591 + 5898 x_B) \text{ J mol}^{-1} \quad (66)$$

and the extent of the miscibility gap, Fig. 25, was $0.284 \leq x_B \leq 0.946$. The calculated eutectic is 123.7 °C, x_B

$= 0.252$. The calculated two-liquid envelope is suggestive only. An uncertainty of $\pm 2^\circ$ may be assigned to the remainder of the diagram.

12.26. Acetanilide (A)+Phenacetin (B)

Data were obtained by DSC.³⁶ Complete solid solution was reported, with a minimum temperature of 80 °C, $x_B = 0.337$. It was found, in preliminary calculations, that all the observed liquidus data were consistent with zero solid solubility and the quantity

$$G^E(l) = x_A x_B (-8900 - 3194 x_B) \text{ J mol}^{-1} \quad (67A)$$

for the liquid. The reason for the thermal event(s) at ~ 82 °C is therefore puzzling. A congruently melting compound in the middle of the diagram could conceivably account for two eutectic temperatures near 82 °C; its stoichiometry, however, could not be 1:1. The presence of an incongruently melting

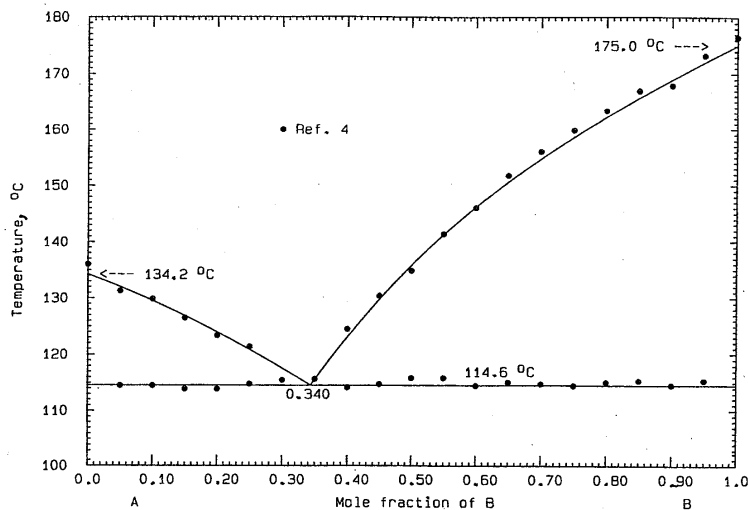


FIG. 27. The system phenacetin (A)+phenobarbital (B).

compound would be equally unlikely. Suggested calculated liquidus curves [Fig. 26(a)] meet at a conjectured eutectic $\sim 60^\circ\text{C}$, $x_B \sim 0.4$.

An alternative construction is possible. The reported³⁶ lowest temperature arrests at $\sim 82^\circ\text{C}$ could be construed as indicating a eutectic temperature; the reported³⁶ "minimum" composition, its composition. In this case, the calculated phase diagram would be that in Fig. 26(b) and the liquid would be described by

$$G^E(l) = x_A x_B (-4090 + 2635 x_B) \text{ J mol}^{-1} \quad (67B)$$

Without further information, a more definitive construction cannot be made.

12.27. Phenacetin (A)+Phenobarbital (B)

Data were obtained by DTA⁴ and the reported eutectic is 114°C , $x_B = 0.33$. All liquidus data were optimized, with the result

$$G^E(l) = x_A x_B (-1600 + 1300 x_B) \text{ J mol}^{-1} \quad (68)$$

and the calculated phase diagram is shown in Fig. 27. The calculated eutectic is 114.6°C , $x_B = 0.340$. An uncertainty of $\pm 2^\circ$ may be assigned to the calculated diagram.

12.28. Paracetamol (A)+Phenobarbital (B)

Data were obtained by DTA,⁴ and the reported eutectic is 141°C , $x_B = 0.45$. Thermal events at about 139°C in the

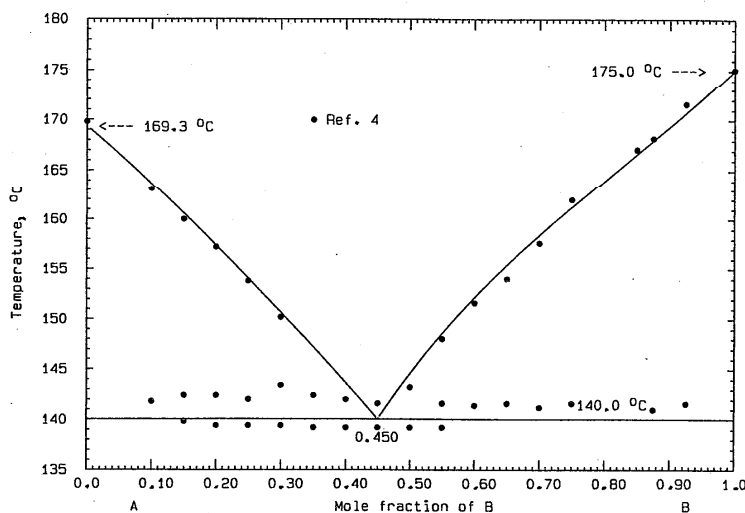


FIG. 28. The system paracetamol (A)+phenobarbital (B).

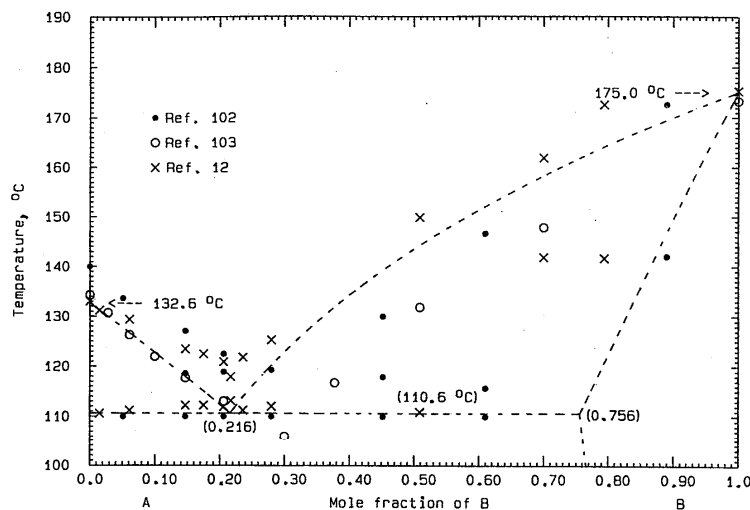


FIG. 29. The system urea (A)+phenobarbital (B). The diagram is conjectural.

range $0.15 < x_B < 0.55$ were ascribed tentatively⁴ to a metastable form of phenobarbital. The liquidus data, upon optimization, proved to be thermodynamically consistent with a eutectic temperature below that observed:

$$G^E(l) = x_A x_B (339 + 1722 x_B) \text{ J mol}^{-1} \quad (69)$$

as shown in the calculated phase diagram (Fig. 28); calculated eutectic: 140.0°C , $x_B = 0.450$. An uncertainty of $\pm 1^\circ$ may be assigned to the calculated diagram.

12.29. Urea (A)+Phenobarbital (B)

Data were obtained by DTA^{12,102} and thermal analysis (cooling curves).¹⁰³ Both physical mixtures¹⁰² and fused samples^{12,102,103} were used (only data for fused mixtures appear in the diagram). The reported eutectic is¹⁰² 111°C , x_B

$= 0.3$ or¹⁰³ 106°C , $x_B = 0.3$ or¹² 112°C , $x_B = 0.22$. Phase diagram data^{12,102} suggested the presence of a solid solution based on phenobarbital; refractive index, photomicrographic analysis and dissolution rate studies¹² also suggested the presence of a solid solution. The limits of the solid solution were given¹² as $0.51 < x_B < 1$ at the eutectic temperature. On the contrary, the phase diagram data and photomicrographic analysis by other investigators¹⁰³ claimed no solid solution.

In addition, the existence of an incongruently melting 1:2 compound was postulated.¹⁰²

Both the data and their interpretation are confused. The phase diagram data themselves are of poor quality. In preliminary calculations, it was ascertained that the high eutectic temperature and lack of eutectic arrests beyond $x_B = 0.6$ were consistent with a solid solution based on phenobarbital;

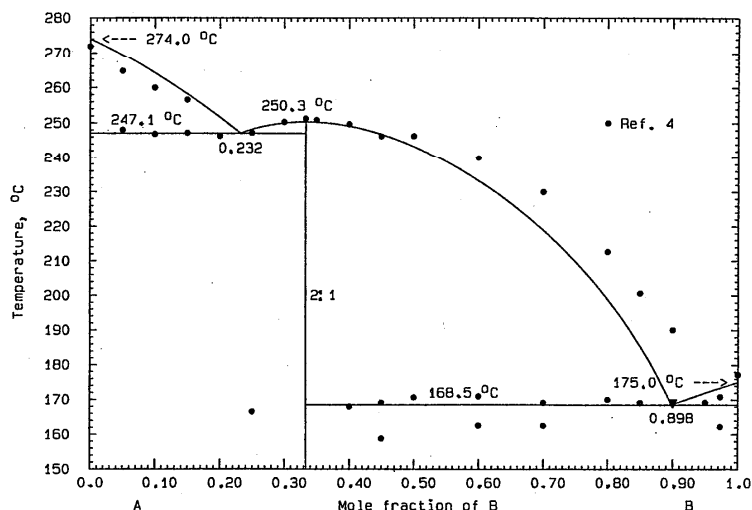


FIG. 30. The system theophylline (A)+phenobarbital (B).

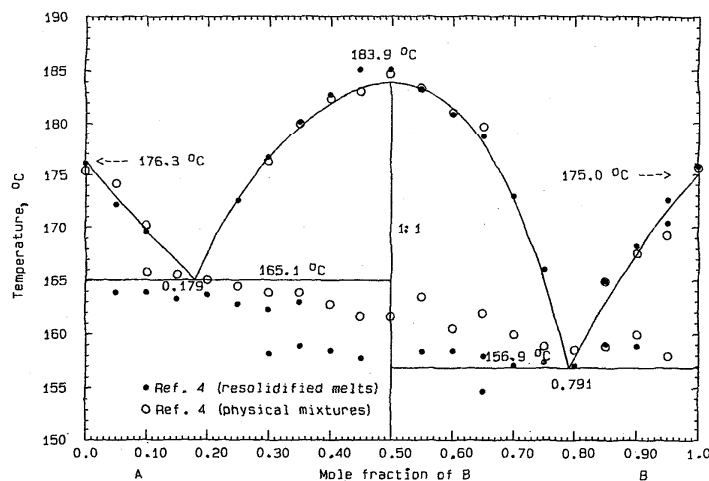


FIG. 31. The system quinine (A)+phenobarbital (B).

there is no justification for the presence of compounds. For construction of the phase diagram, Eq. (70) was assumed

$$G^E(l) = 0, \quad (70)$$

and the solid solution was assumed to be Henrian; the Henrian activity coefficient

$$RT \ln \gamma_A = 4500 \text{ J mol}^{-1} \quad (71)$$

independent of temperature was chosen in order to place the eutectic temperature near the observed data points. The calculated phase diagram is shown in Fig. 29, and the calculated eutectic is 110.6 °C, $x_B = 0.216$. The solid solution extends to $x_B = 0.756$ at the eutectic temperature. The diagram is suggestive only.

12.30. Theophylline (A)+Phenobarbital (B)

Data were obtained by DTA⁴ and the microthermal method¹⁰⁴ (smooth line diagram, no data points). The reported eutectics⁴ are $E_1 = 248$ °C, $x_B = 0.25$ and $E_2 = 169$ °C, $x_B = 0.96$. There is a 2:1 compound melting congruently at⁴ 252 °C. The x-ray diffraction spectra of mixtures⁴ at $x_B = 0.33$ and 0.4 support the existence of a compound. The 2:1 compound was synthesized from alcohol solution¹⁰⁵ with a melting point of 250.7–251.7 °C. Another report¹⁰⁴ indicates the existence of 1:1 and 2:1 compounds melting at 254 and 244 °C, respectively. Some thermal events in the range⁴ 159–164 °C were thought to be due to metastable transitions of phenobarbital.

A preliminary calculation showed that liquidus data⁴ at $x_B > 0.6$ were inaccurate and no compound was thermodynamically stable. The phase diagram, Fig. 30, was calculated with the use of Eq. (72)

$$G^E(l) = x_A x_B (-4667 + 2000 x_B) \text{ J mol}^{-1} \quad (72)$$

for the liquid and, for the compound $A_2B/2$,

$$\Delta_{\text{fus}} G^o = 26563 - 50.7801T \text{ J mol}^{-1}, \quad (73)$$

$$\Delta_f G^o = -27452 + 45.4498T \text{ J mol}^{-1}. \quad (74)$$

Other calculated data are: $E_1 = 247.1$ °C, $x_B = 0.232$ and $E_2 = 168.5$ °C, $x_B = 0.898$. The compound melts at 250.3 °C. An uncertainty of ± 4 ° may be assigned to the calculated diagram.

12.31. Quinine (A)+Phenobarbital (B)

Data were obtained from DTA measurements on both physical and fused mixtures.⁴ The reported eutectics⁴ (fused mixtures) are $E_1 = 164$ °C, $x_B = 0.2$ and $E_2 = 158$ °C, $x_B = 0.8$. A 1:1 compound melts congruently at 185 °C. The liquidus data from the physical and fused mixtures agree quite well; the two preparative methods give different eutectic temperatures, however. There is a metastable eutectic in the range 120–130 °C. X-ray diffraction spectra⁴ on the powder confirmed the existence of the 1:1 compound. The compound was also synthesized from alcohol solution^{7,106} and melted at¹⁰⁶ 182–183 °C or⁷ 184–185 °C. The eutectic arrests⁴ were scattered, and preliminary calculations showed that both eutectic temperatures from fused mixtures could not be reproduced simultaneously. In this case, it was decided to place more weight on the liquidus data; the optimization yielded

$$G^E(l) = x_A x_B (1329 - 5010 x_B) \text{ J mol}^{-1}, \quad (75)$$

for the liquid and

$$\Delta_{\text{fus}} G^o = 18377 - 40.2038T \text{ J mol}^{-1}, \quad (76)$$

$$\Delta_f G^o = -18671 + 34.4426T \text{ J mol}^{-1} \quad (77)$$

for the compound $AB/2$. Calculated data from the phase diagram, Fig. 31, are $E_1 = 165.1$ °C, $x_B = 0.179$ and $E_2 = 156.9$ °C, $x_B = 0.791$. The compound melts at 183.9 °C. The experimental liquidus data are fitted well (uncertainty ± 2 °), but a large uncertainty remains for the eutectics.

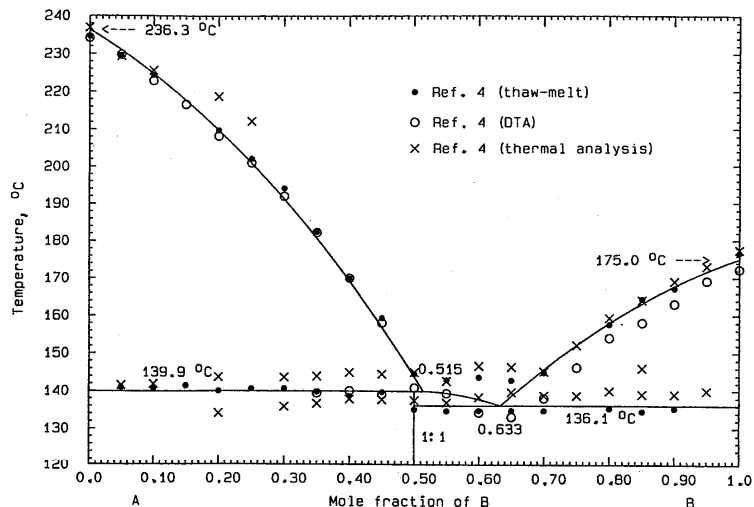


FIG. 32. The system caffeine (A)+phenobarbital (B).

12.32. Caffeine (A)+Phenobarbital (B)

Data were obtained by thermal analysis, DTA and the thaw-melt method.⁴ The 1:1 compound is described as⁴ “incongruently melting” but reference is made exclusively to two “eutectic” temperatures (the higher should be called “peritectic”). Thermal events between 120 and 130 °C were ascribed⁴ to metastable eutectics. The eutectic⁴ is 135 (or 138) °C, $x_B=0.67$ and the peritectic temperature is 140, 141 or 143 °C. A 1:2 compound was prepared¹⁰⁷ from aqueous solution (melting point 145–146 °C) as well as a 1:1 compound (not isolated). Liquidus data from all three methods agree well on the LHS, and, on the RHS, the DTA and thaw-melt data are concordant; in the central region there is much scatter. All liquidus data in the intervals $0 < x_B < 0.5$ and $0.7 < x_B < 1$ were optimized, with the result

$$G^E(l) = -6377x_Ax_B \text{ J mol}^{-1} \quad (78)$$

for the liquid and

$$\Delta_{\text{fus}}G^o = 25\,380 - 61.4325T \text{ J mol}^{-1}, \quad (79)$$

$$\Delta_fG^o = -26\,975 + 55.6714T \text{ J mol}^{-1} \quad (80)$$

for the compound AB/2. The phase diagram, calculated with the use of Eqs. (78) and (80), is shown in Fig. 32; other calculated data are $E=136.1$ °C, $x_B=0.633$ and $P=139.9$ °C, $x_B=0.515$. An uncertainty of $\pm 4^\circ$ may be assigned to the calculated diagram.

12.33. Aspirin (A)+Phenobarbital (B)

Data were obtained from DTA⁴ and the reported eutectic is 122 °C, $x_B=0.35$. The eutectic data are, in fact, scattered, but the liquidus data are not. Optimization of the liquidus data yielded the quantity

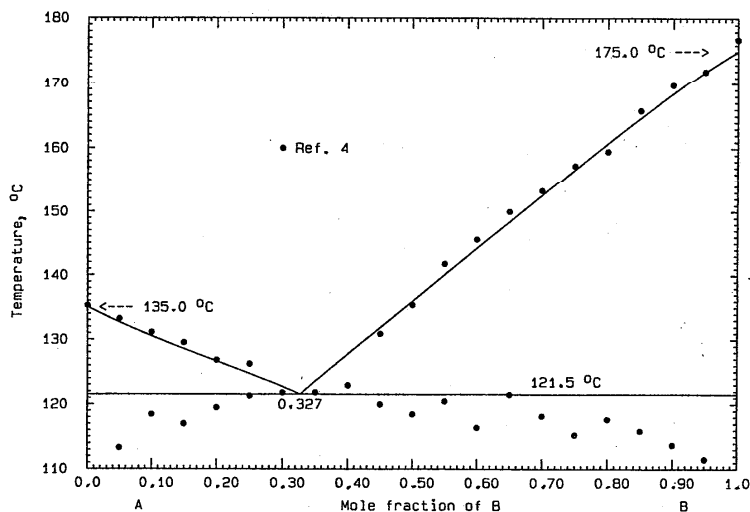


FIG. 33. The system aspirin (A)+phenobarbital (B).

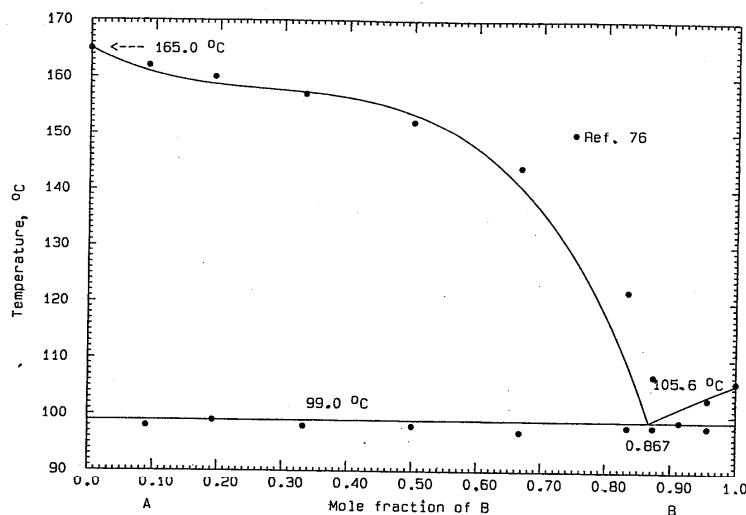


FIG. 34. The system sulfanilamide (A)+phenylbutazone (B).

$$G^E(l) = x_A x_B (2714 - 2978 x_B) \text{ J mol}^{-1} \quad (81)$$

and the calculated phase diagram, Fig. 33, shows a eutectic 121.5°C , $x_B = 0.327$. An uncertainty of $\pm 1^\circ$ may be assigned to the diagram.

12.34. Sulfanilamide (A)+Phenylbutazone (B)

Data were obtained by DSC and light transmission.⁷⁶ The reported eutectic is 99°C , $x_B = 0.91$. X-ray diffractograms of mixtures corresponded to the two components only. The liquidus data by themselves entail a eutectic temperature somewhat higher than that observed. Weighting the eutectic temperature preferentially, the optimization yielded

$$G^E(l) = x_A x_B (7016 - 5500 x_B) \text{ J mol}^{-1} \quad (82)$$

and the calculated phase diagram, Fig. 34, shows a eutectic

99.0°C , $x_B = 0.867$. The rather high-lying liquidus suggests incipient liquid immiscibility. An uncertainty of $\pm 2^\circ$ may be assigned to the calculated diagram.

12.35. Khellin (A)+Sulfanilamide (B)

Data were obtained by DSC, DTA and the microthermal method.⁸² Data from the three methods were concordant and not all are shown on the diagram. The reported eutectics are $E_1 = 141^\circ\text{C}$, $x_B = 0.23$ and $E_2 = 146.5^\circ\text{C}$, $x_B = 0.74$; the 1:1 compound melts congruently at 151.5°C . The diagram as a whole could be well reproduced with the quantities

$$G^E(l) = 207 x_A x_B \text{ J mol}^{-1} \quad (83)$$

and

$$\Delta_{\text{fus}} G^\circ = 24452 - 57.5227T \text{ J mol}^{-1}, \quad (84)$$

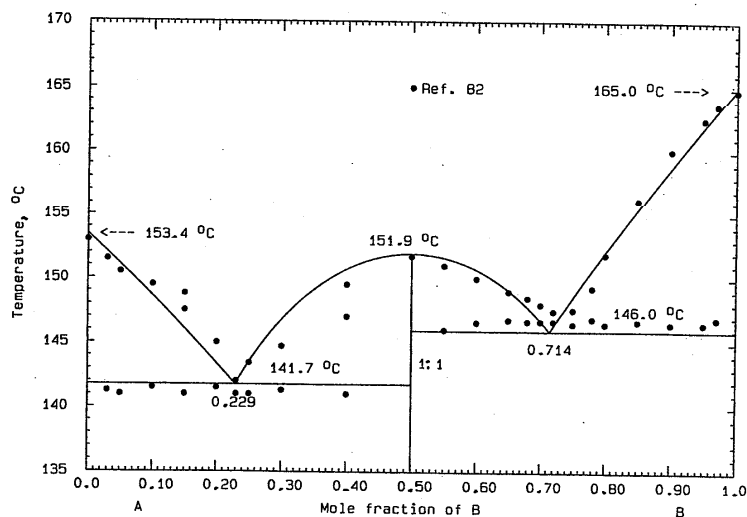


FIG. 35. The system khellin (A)+sulfanilamide (B).

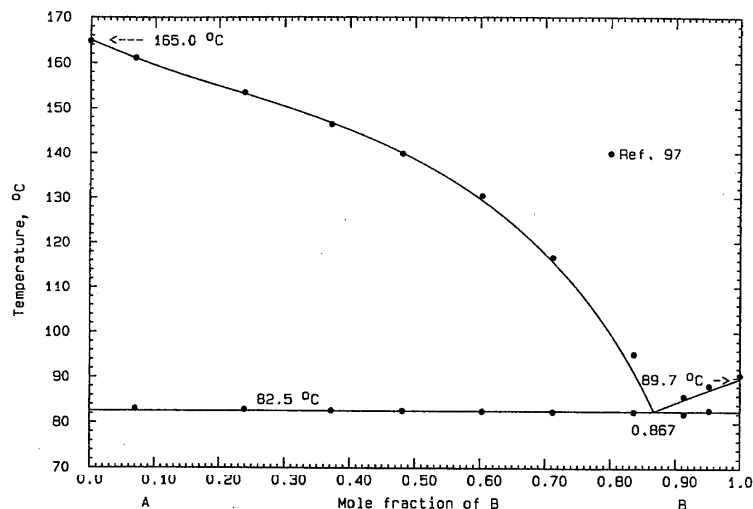


FIG. 36. The system sulfanilamide (A)+benzocaine (B).

$$\Delta_f G^o = -24400 + 51.7615T \quad \text{J mol}^{-1} \quad (85)$$

for the compound AB/2. The calculated phase diagram is shown in Fig. 35, and other calculated data are $E_1 = 141.7^\circ\text{C}$, $x_B = 0.229$ and $E_2 = 146.0^\circ\text{C}$, $x_B = 0.714$. The compound melts at 151.9°C . A few liquidus data points are seen to be inconsistent with the rest of the diagram. An uncertainty of $\pm 1^\circ$ may be assigned to the calculated diagram.

12.36. Sulfanilamide (A)+Benzocaine (B)

Data were obtained by the thaw-melt method.⁹⁷ The reported eutectic is 82.5°C , $x_B = 0.87$. The phase diagram, Fig. 36, was calculated with the aid of

$$G^E(l) = x_A x_B (3128 - 2500x_B) \quad \text{J mol}^{-1} \quad (86)$$

and shows a eutectic of 82.5°C , $x_B = 0.867$. An uncertainty of $\pm 1^\circ$ may be assigned to the calculated diagram.

12.37. Sulfanilamide (A)+4-Aminobenzoic Acid (B)

Data were obtained by the thaw-melt method⁹⁷ and the reported eutectic is 138.5°C , $x_B = 0.38$. The phase diagram, Fig. 37, was calculated with the use of Eq. (87)

$$G^E(l) = x_A x_B (1200 + 885x_B) \quad \text{J mol}^{-1} \quad (87)$$

and shows a eutectic 138.6°C , $x_B = 0.404$. Two liquidus data near $x_B = 0.4$ are seen to be inconsistent with the remaining data. An uncertainty of $\pm 1^\circ$ may be assigned to the calculated diagram.

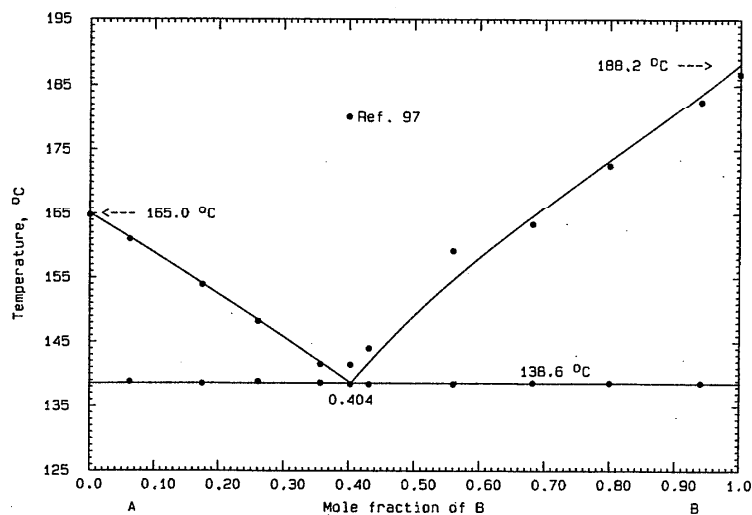


FIG. 37. The system sulfanilamide (A)+4-aminobenzoic acid (B).

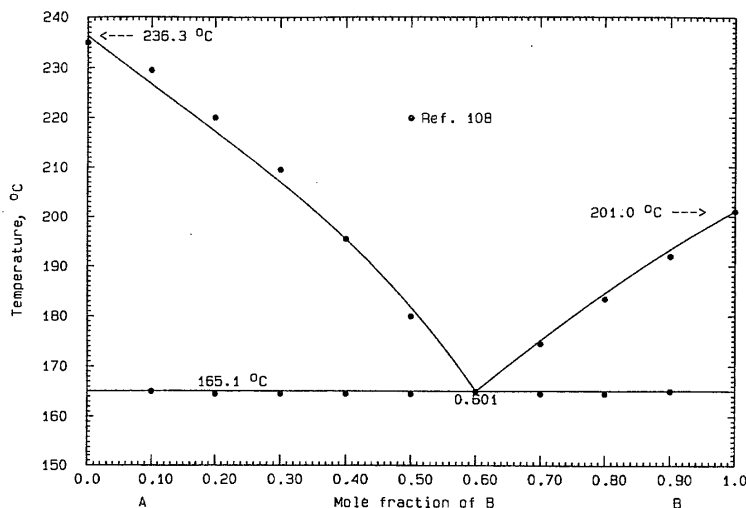


FIG. 38. The system caffeine (A)+sulfathiazole (B).

12.38. Caffeine (A)+Sulfathiazole (B)

Data were obtained by DSC and light transmission.¹⁰⁸ The reported eutectic is 165 °C, $x_B=0.6$. X-ray diffraction of mixtures confirmed the fact that the system is a simple eutectic. (A stability constant for an associated species in aqueous solution was derived from solubility measurements:¹⁰⁷ at 30 °C.) All liquidus data were optimized to give Eq. (88)

$$G^E(l) = x_A x_B (1073 - 1639 x_B) \text{ J mol}^{-1} \text{ K}^{-1} \quad (88)$$

with which the phase diagram, Fig. 38, was calculated. The calculated eutectic is 165.1 °C, $x_B=0.601$. An uncertainty of $\pm 1^\circ$ may be assigned to the calculated diagram.

12.39. Sulfathiazole (A)+Phenylbutazone (B)

Data were obtained by DSC and light transmission.⁷⁶ The reported eutectic is 103 °C, $x_B=0.98$ and peritectic 160 °C,

$x_B=0.49$. X-ray diffraction data on the 2:1 compound at room temperature were indexed according to triclinic symmetry, with $a=1.0403$ nm, $b=1.0673$ nm, $c=1.9628$ nm, $\alpha=82.21^\circ$, $\beta=99.98^\circ$, $\gamma=102.36^\circ$, $Z=2$. The compound undergoes a transition at 150 °C, and unindexed diffraction data were obtained for the high temperature form. A metastable eutectic was observed at 94 °C. All liquidus data were optimized, with the results

$$G^E(l) = x_A x_B (690 + 1500 x_B - 2500 x_B^2) \text{ J mol}^{-1}, \quad (89)$$

and

$$\Delta_{\text{fus}} G^\circ = 16\,106 - 36.7147T \text{ J mol}^{-1}, \quad (90)$$

$$\Delta_f G^\circ = -15\,903 + 31.4227T \text{ J mol}^{-1} \quad (91)$$

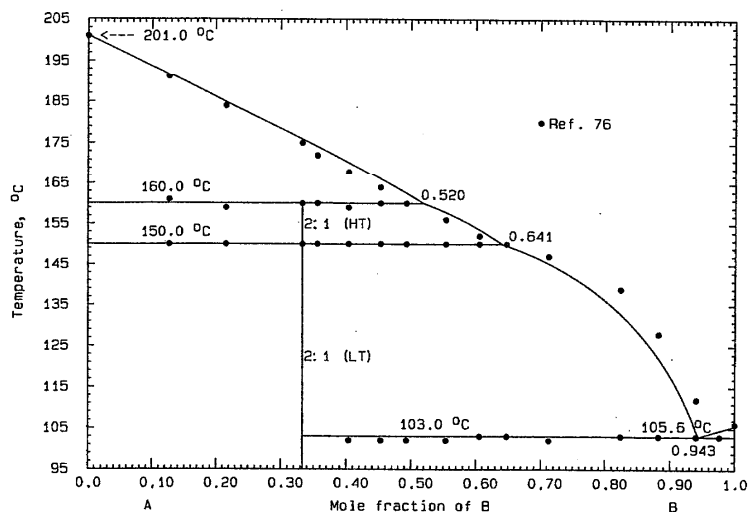


FIG. 39. The system sulfathiazole (A)+phenylbutazone (B).

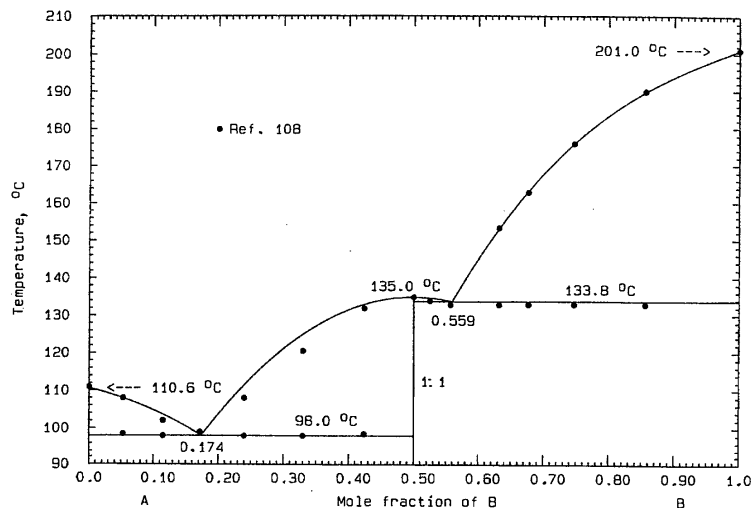


FIG. 40. The system phenazone (A)+sulfathiazole (B).

for the compound $A_2B/3$. The calculated enthalpy of transition of the compound is $17\,241\text{ J mol}^{-1}$. The calculated phase diagram is shown in Fig. 39, and calculated data $E = 103.0^\circ\text{C}$, $x_B = 0.943$; $P = 160.0^\circ\text{C}$, $x_B = 0.520$. The calculated transition appears on the liquidus at 150.0°C , $x_B = 0.641$. An uncertainty of $\pm 1^\circ$ may be assigned to the calculated diagram.

12.40. Phenazone (A)+Sulfathiazole (B)

Data were obtained by DSC and light transmission.¹⁰⁸ The reported eutectics are $E_1 = 99^\circ\text{C}$, $x_B = 0.17$ and $E_2 = 133^\circ\text{C}$, $x_B = 0.53$. The 1:1 compound melts congruently at 135°C . X-ray diffraction data on the compound were indexed according to monoclinic symmetry: $a = 1.2669\text{ nm}$, b

$= 1.2590\text{ nm}$, $c = 1.3941\text{ nm}$, $\beta = 105.18^\circ$, $Z = 4$, space group $P2_1/c$. All liquidus data were optimized with the result

$$G^E(l) = x_A x_B (-11\,346 - 5387x_B + 8769x_B^2) \text{ J mol}^{-1} \quad (92)$$

for the liquid and

$$\Delta_{\text{fus}}G^\circ = 25\,155 - 61.6288T \text{ J mol}^{-1}, \quad (93)$$

$$\Delta_f G^\circ = -28\,117 + 55.8677T \text{ J mol}^{-1} \quad (94)$$

for the compound $AB/2$. The calculated phase diagram is shown in Fig. 40, with eutectics $E_1 = 98.0^\circ\text{C}$, $x_B = 0.174$; $E_2 = 133.8^\circ\text{C}$, $x_B = 0.559$. The compound melts at 135.0°C . An uncertainty of $\pm 1^\circ$ may be assigned to the calculated diagram.

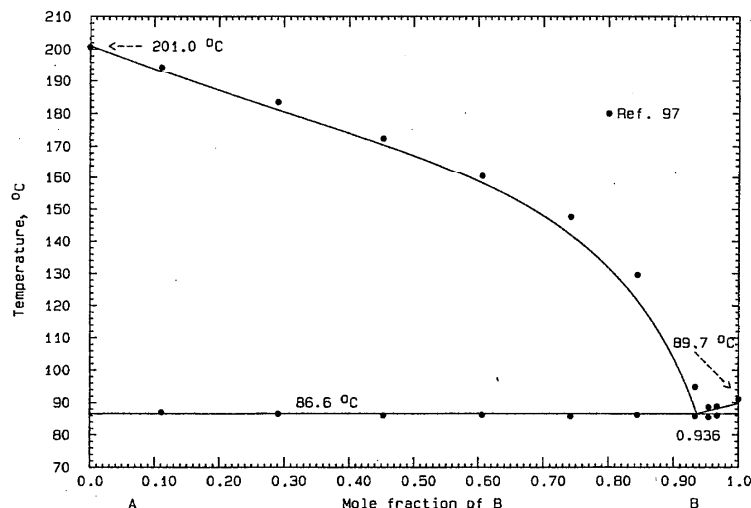


FIG. 41. The system sulfathiazole (A)+benzocaine (B).

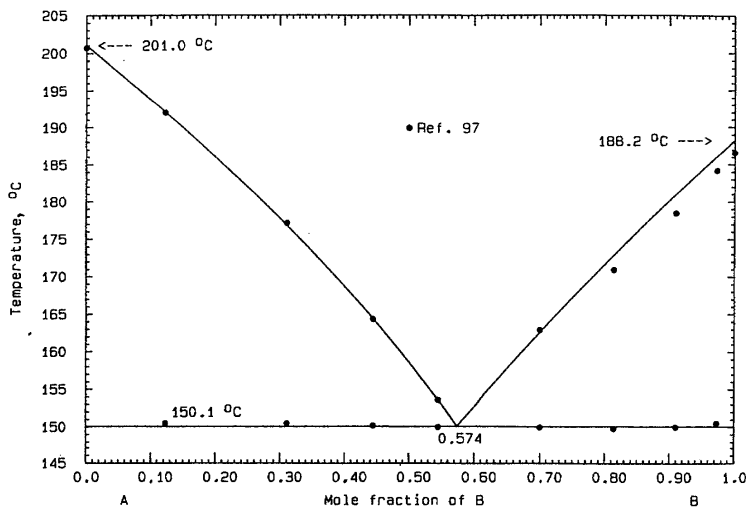


Fig. 12. The system sulfathiazole (A)+4-aminobenzoic acid (B).

12.41. Sulfathiazole (A)+Benzocaine (B)

Data were obtained by the thaw-melt method⁹⁷ and the reported eutectic is 86 °C, $x_B=0.96$. In a preliminary calculation, it was ascertained that the liquidus data were consistent with a eutectic temperature slightly above that observed. The phase diagram, Fig. 41, was calculated with the use of Eq. (95).

$$G^E(l) = x_A x_B (2200 + 1157 x_B - 1477 x_B^2) \text{ J mol}^{-1} \quad (95)$$

and shows a calculated eutectic of 86.6 °C, $x_B=0.936$. An uncertainty of $\pm 2^\circ$ may be assigned to the calculated diagram.

12.42. Sulfathiazole (A)+4-Aminobenzoic Acid (B)

Data were obtained by the thaw-melt method⁹⁷ and the reported eutectic is 150 °C, $x_B=0.57$. All data were optimized to give the expression

$$G^E(l) = 507 x_A x_B \text{ J mol}^{-1} \quad (96)$$

and the calculated phase diagram appears in Fig. 42. The calculated eutectic is 150.1 °C, $x_B=0.574$. A few experimental liquidus points are obviously faulty. An uncertainty of $\pm 1^\circ$ may be assigned to the calculated diagram.

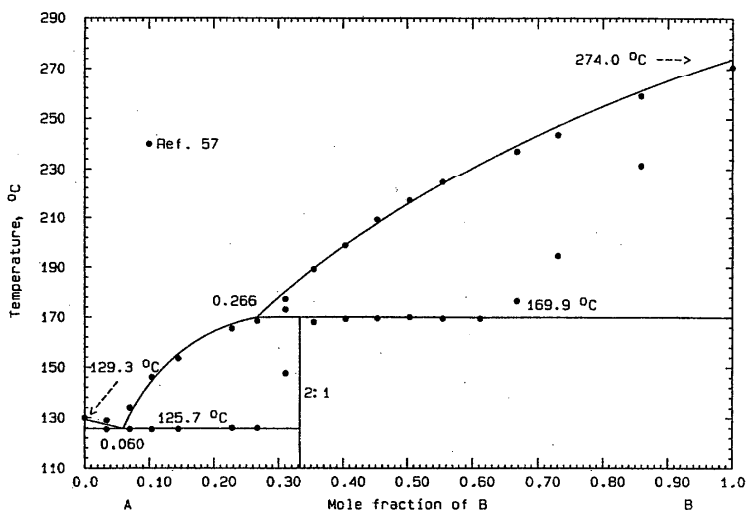


Fig. 43. The system nicotinamide (A)+theophylline (B).

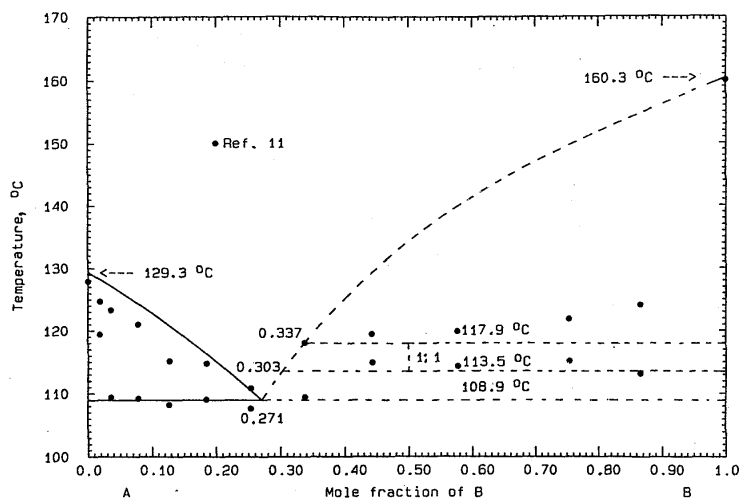


FIG. 44. The system nicotinamide (A)+indomethacin (B). Most of the diagram is conjectural.

12.43. Nicotinamide (A)+Theophylline (B)

Data were obtained by the thaw-melt method on physical and fused mixtures⁵⁷ (only data for fused mixtures are shown on the diagram). No invariant points were mentioned, but there is an incongruently melting 2:1 compound. All liquidus data were optimized and Eq. (97)

$$G^E(l) = -1377x_Ax_B \quad \text{J mol}^{-1} \quad (97)$$

represented the liquid and

$$\Delta_{\text{fus}}G^\circ = 12006 - 27.0777T \quad \text{J mol}^{-1}, \quad (98)$$

$$\Delta_{\text{f}}G^\circ = -12350 + 21.7892T \quad \text{J mol}^{-1} \quad (99)$$

the compound $A_2B/3$. The calculated phase diagram appears in Fig. 43 and other calculated data are $E = 125.7^\circ\text{C}$, $x_B = 0.060$; $P = 169.9^\circ\text{C}$, $x_B = 0.266$. An uncertainty of $\pm 3^\circ$ may be assigned to the calculated diagram.

12.44. Nicotinamide (A)+Indomethacin (B)

Data were obtained by hot-stage microscopy.¹¹ Samples were prepared from fused mixtures and two (of 5 and 10 wt %) from solvent-evaporated mixtures. A metastable eutectic at 83°C and a stable one at 107°C were reported. A solid solution based on nicotinamide was postulated, together with two incongruently melting compounds (1:1 and 1:2). IR

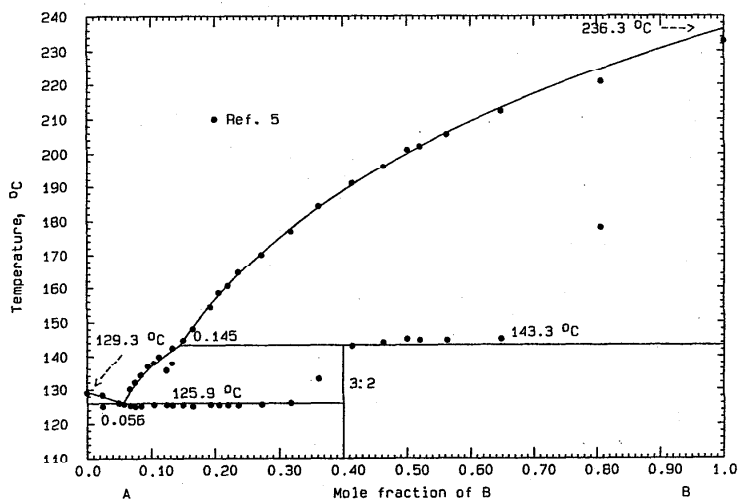


FIG. 45. The system nicotinamide (A)+sulfamerazine (B).

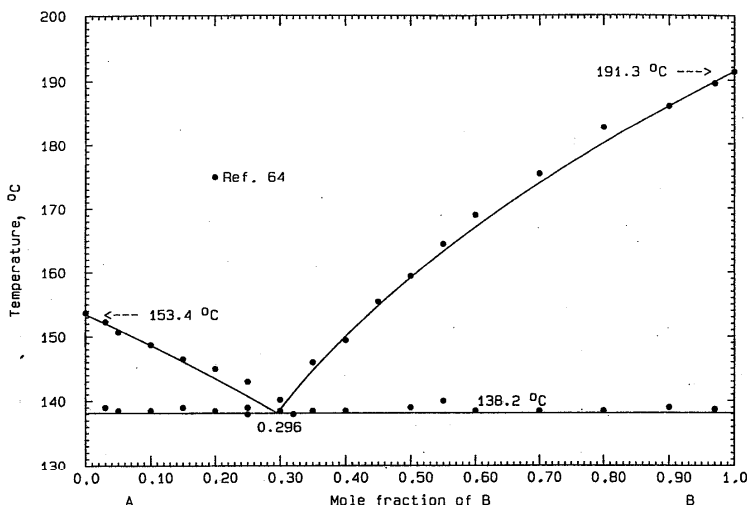


FIG. 46. The system khellin (A)+sulfapyridine (B).

spectra of mixtures and UV spectra of aqueous mixtures were claimed to yield results confirming the existence of complexes, as did solubility studies.

The liquidus data are sparse and of poor quality. Preliminary calculations showed that a solid solution based on nicotinamide was not needed. For construction of a phase diagram a eutectic temperature near 107 °C was assumed. A 1:1 compound proved to be possible thermodynamically, but stable only in a narrow temperature range. For the liquid, Eq. (100) was used

$$G^E(l) = x_A x_B (-1475 + 1933 x_B) \text{ J mol}^{-1} \quad (100)$$

and for the compound AB/2

$$\Delta_{\text{fus}} G^{\circ} = 9787 - 24.4798T \text{ J mol}^{-1}, \quad (101)$$

$$\Delta_f G^{\circ} = -9914 + 18.7186T \text{ J mol}^{-1}. \quad (102)$$

The calculated phase diagram appears in Fig. 44. The calculated eutectic is 108.9 °C, $x_B = 0.271$; the two peritectics are 113.5 °C, $x_B = 0.303$ and 117.9 °C, $x_B = 0.337$. The behavior of the compound is consistent with the presence of two observed peritectic temperatures, but the diagram remains conjectural.

12.45. Nicotinamide (A)+Sulfamerazine (B)

Data were obtained by the thaw-melt method.⁵ Physical, fused and solvent-evaporated mixtures were used. Only data from fused mixtures are shown in the diagram. No invariant points were stated, but a metastable eutectic at 123 °C was reported and also the presence of an incongruently melting

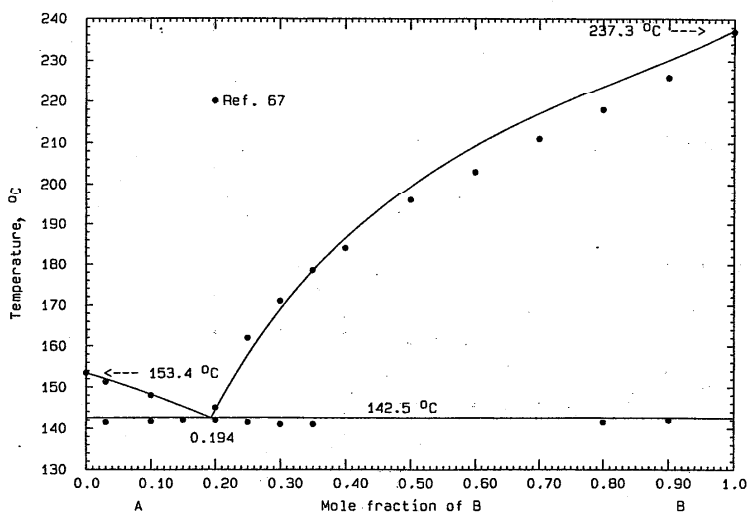


FIG. 47. The system khellin (A)+nicotinic acid (B).

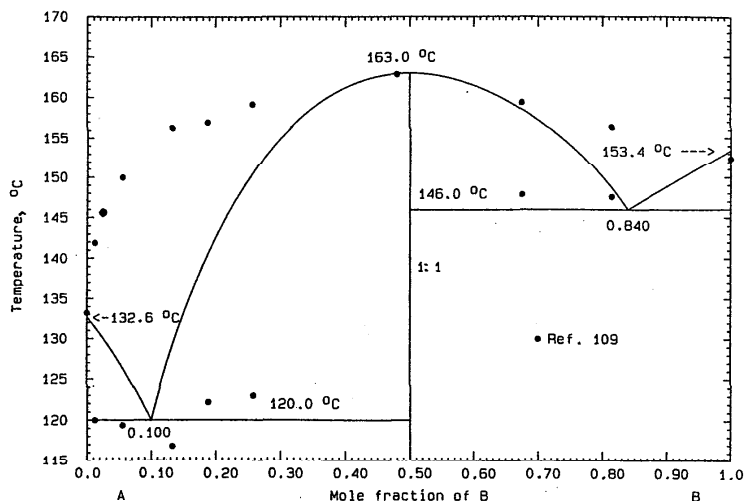


FIG. 48. The system urea (A)+khellin (B).

3:2 compound. The compound was synthesized in and isolated from acetone solution. All liquidus data from fused mixtures were optimized, with the result

$$G^E(l) - x_A x_B (-688 + 517x_B) \text{ J mol}^{-1} \quad (103)$$

for the liquid and

$$\Delta_{\text{fus}} G^\circ = 26955 - 62.9912T \text{ J mol}^{-1}, \quad (104)$$

$$\Delta_f G^\circ = -27071 + 57.3974T \text{ J mol}^{-1} \quad (105)$$

for the compound $A_3B_2/5$. The calculated phased diagram is shown in Fig. 45. Calculated data are $E=125.9^\circ\text{C}$, $x_B=0.056$ and $P=143.3^\circ\text{C}$, $x_B=0.145$. An uncertainty of $\pm 1^\circ$ may be assigned to the calculated diagram.

12.46. Khellin (A)+Sulfapyridine (B)

Data were obtained by DTA, DSC and light transmission;⁶⁴ results from the three methods were concordant. The reported eutectic is 138.5°C , $x_B=0.32$. Samples were also examined photomicrographically. Optimization of the liquidus data yielded the expression

$$G^E(l) = 461x_A x_B \text{ J mol}^{-1}, \quad (106)$$

and the phase diagram calculated with this quantity is shown in Fig. 46. The calculated eutectic is 138.2°C , $x_B=0.296$. An uncertainty of $\pm 2^\circ$ may be assigned to the calculated diagram.

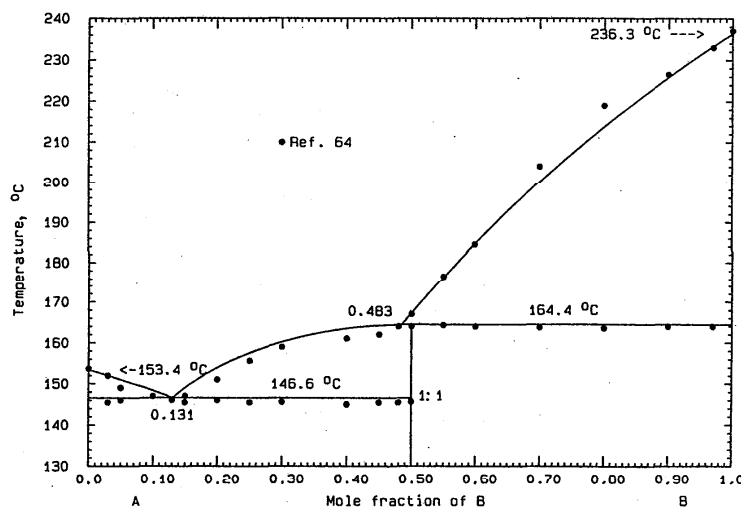


FIG. 49. The system khellin (A)+caffeine (B).

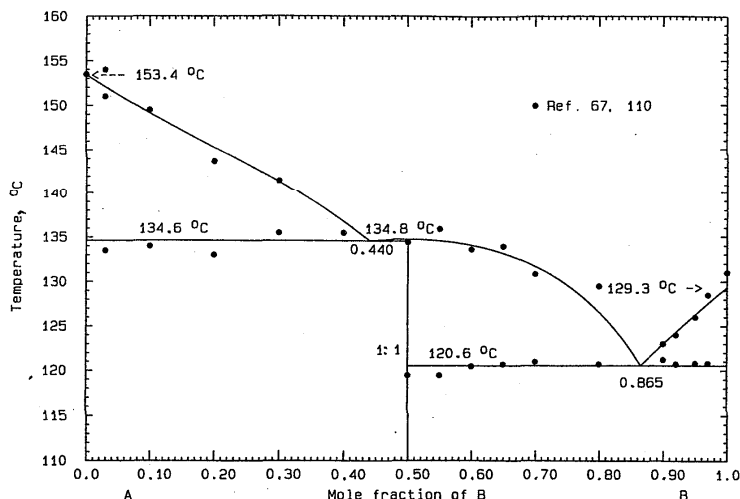


FIG. 50. The system khellin (A)+nicotinamide (B).

12.47. Khellin (A)+Nicotinic Acid (B)

Data were obtained by DSC and thermal microscopy⁶⁷ and results from both methods are in good agreement. The same data are reported elsewhere.¹⁰⁹ The reported eutectic is 142 °C, $x_B=0.18$. Samples were also examined photomicroscopically. Nicotinic acid displayed a solid transformation at 184 °C (not shown on the diagram). The liquidus data were optimized to give

$$G^E(l) = x_A x_B (-400 + 3000 x_B) \text{ J mol}^{-1}, \quad (107)$$

and the phase diagram calculated with this quantity is shown in Fig. 47. The calculated eutectic is 142.5 °C, $x_B=0.194$. The RHS experimental liquidus data show erratic changes of slope; the calculated liquidus is probably closer to true behavior. An uncertainty of $\pm 4^\circ$ may be assigned to the calculated diagram.

12.48. Urea (A)+Khellin (B)

Data were obtained by DTA and the Boetius microheating table.¹⁰⁹ Two eutectic temperatures were reported: 120 and 146 °C; the existence of a congruently melting 1:1 compound (163 °C) was also suggested. Although the data are very scattered, it proved possible to construct a reasonable phase diagram with the use of Eq. (108)

$$G^E(l) = x_A x_B (-6350 + 4800 x_B) \text{ J mol}^{-1} \quad (108)$$

for the liquid and

$$\Delta_{\text{fus}} G^\circ = 29\,617 - 67.8994T \text{ J mol}^{-1}, \quad (109)$$

$$\Delta_f G^\circ = -30\,605 + 62.1366T \text{ J mol}^{-1} \quad (110)$$

for the compound AB/2. The calculated phase diagram is shown in Fig. 48. The calculated eutectics are $E_1=120.0^\circ\text{C}$, $x_B=0.100$ and $E_2=146.0^\circ\text{C}$, $x_B=0.840$. The compound melts at 163.0 °C. An uncertainty of $\pm 10^\circ$ may be assigned to the calculated diagram.

12.49. Khellin (A)+Caffeine (B)

Data were obtained by DSC, DTA and thermal microscopy.⁶⁴ The data for the three methods are in good agreement. The reported eutectic is 146.0 °C, $x_B=0.13$ and peritectic 164.5 °C, $x_B=0.48$ (1:1 compound). Samples were also examined by photomicroscopy. The best fit to the data was obtained with the use of Eq. (111) for the liquid

$$G^E(l) = -1784 x_A x_B \text{ J mol}^{-1}, \quad (111)$$

and

$$\Delta_{\text{fus}} G^\circ = 39\,554 - 90.3864T \text{ J mol}^{-1}, \quad (112)$$

$$\Delta_f G^\circ = -40\,000 + 84.6252T \text{ J mol}^{-1} \quad (113)$$

for the compound AB/2. The calculated phase diagram is given in Fig. 49; other calculated data are $E=146.6^\circ\text{C}$, $x_B=0.131$ and $P=164.4^\circ\text{C}$, $x_B=0.483$. An uncertainty of $\pm 2^\circ$ may be assigned to the calculated diagram.

12.50. Khellin (A)+Nicotinamide (B)

Data were obtained by DSC and thermomicroscopy.^{67,110} The two methods gave concordant results. The existence of a 1:1 compound was demonstrated by x-ray diffraction measurements; in the report, it is described as melting incongruently ($P=133^\circ\text{C}$, $x_B=0.5$). From the liquidus data themselves, however, it is difficult, if not impossible, to ascertain whether the compound melts congruently or incongruently. In preliminary calculations, it became evident that the liquidus data were thermodynamically consistent with a congruent melting behavior. The excess Gibbs energy of the liquid is given by

$$G^E(l) = x_A x_B (2500 - 1100 x_B) \text{ J mol}^{-1}, \quad (114)$$

and the compound AB/2 is represented by

$$\Delta_{\text{fus}} G^\circ = 37\,872 - 92.8271T \text{ J mol}^{-1}, \quad (115)$$

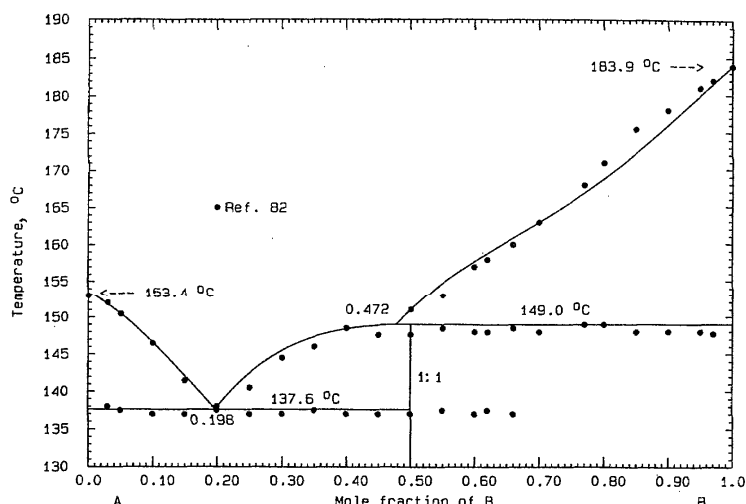


FIG. 51. The system khellin (A)+sulfacetamide (B).

$$\Delta_f G^\circ = -37384 + 87.0660T \quad \text{J mol}^{-1} \quad (116)$$

The calculated phase diagram appears in Fig. 50. The calculated eutectics are $E_1 = 134.6^\circ\text{C}$, $x_B = 0.440$ and $E_2 = 120.6^\circ\text{C}$, $x_B = 0.865$. The melting point of the compound is 134.8°C , almost identical to the E_1 temperature. An uncertainty of $\pm 2^\circ$ may be assigned to the calculated diagram.

12.51. Khellin (A)+Sulfacetamide (B)

Data were obtained by DSC, DTA and thermal microscopy.⁸² Samples were also examined by photomicroscopy. There is a 1:1 compound melting incongruently ($P = 149^\circ\text{C}$, $x_B = 0.45$; $E = 137.5^\circ\text{C}$, $x_B = 0.21$). A metastable eutectic at 124°C was also reported. As presented, the RHS liquidus data impart a peculiar kinked shape to the curve there; the RHS data, in fact, suggest strong positive nonideality in the liquid. The LHS liquidus is normal. The quantity

$$G^E(l) = x_A x_B (-4916 + 14758x_B - 8695x_B^2) \quad \text{J mol}^{-1} \quad (117)$$

allowed the RHS liquidus kink to be approximated. For the compound AB/2,

$$\Delta_{\text{fus}} G^\circ = 40772 - 96.5716T \quad \text{J mol}^{-1}, \quad (118)$$

$$\Delta_f G^\circ = -40700 + 90.8104T \quad \text{J mol}^{-1}. \quad (119)$$

The calculated phase diagram is shown in Fig. 51. Calculated data are $E = 137.6^\circ\text{C}$, $x_B = 0.198$ and $P = 149.0^\circ\text{C}$, $x_B = 0.472$. The true shape of the RHS liquidus may be different. An uncertainty of $\pm 3^\circ$ may be assigned to the calculated diagram.

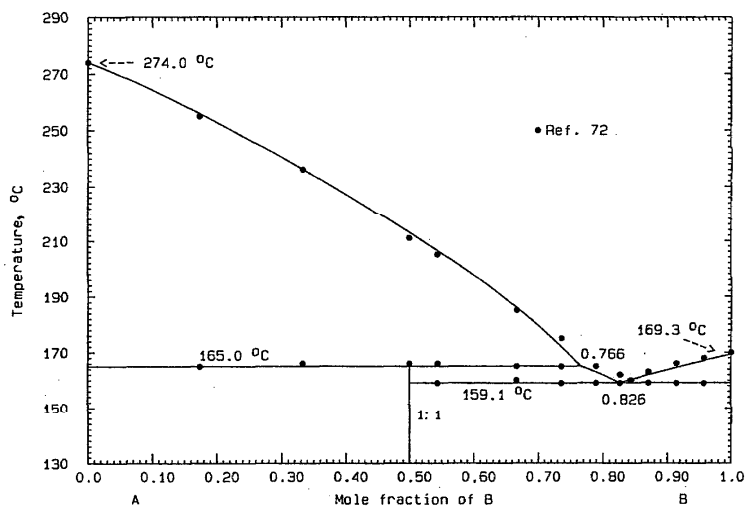


FIG. 52. The system theophylline (A)+paracetamol (B).

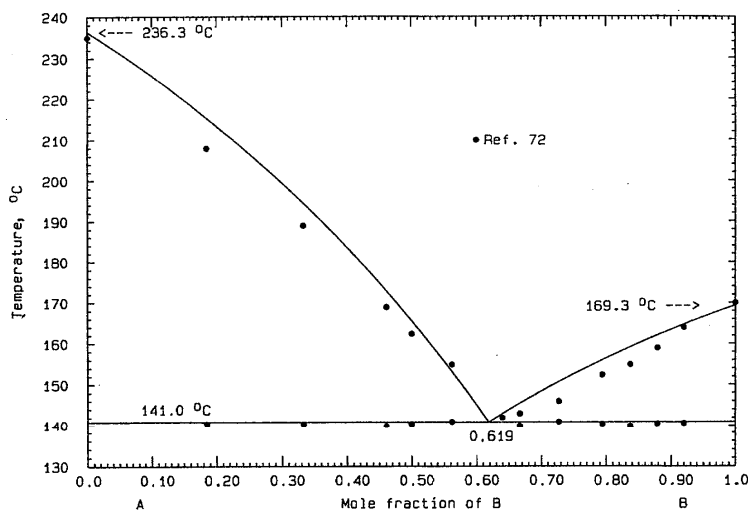


FIG. 53. The system caffeine (A)+paracetamol (B).

12.52. Theophylline (A)+Paracetamol (B)

Data were obtained by DSC and light transmission.⁷² X-ray diffractograms of solid samples indicated the presence of a 1:1 compound melting incongruently. The reported invariant points are $E=159\text{ }^\circ\text{C}$, $x_B=0.84$ and $P=165\text{ }^\circ\text{C}$, $x_B=0.79$. The data could be well represented by

$$G^E(l) = x_A x_B (-2445 + 3586x_B - 2000x_B^2) \text{ J mol}^{-1} \quad (120)$$

for the liquid and

$$\Delta_{\text{fus}}G^o = 30\,062 - 67.1840T \text{ J mol}^{-1}, \quad (121)$$

$$\Delta_f G^o = -30\,350 + 61.4212T \text{ J mol}^{-1} \quad (122)$$

for the compound AB/2. The calculated phase diagram is shown in Fig. 52, with calculated invariant points E

$=159.1\text{ }^\circ\text{C}$, $x_B=0.826$ and $P=165.0\text{ }^\circ\text{C}$, $x_B=0.766$. An uncertainty of $\pm 2^\circ$ may be assigned to the calculated diagram.

12.53. Caffeine (A)+Paracetamol (B)

Data were obtained by DSC and light transmission.⁷² X-ray diffractograms of solid samples showed the system to be a simple eutectic ($E=142\text{ }^\circ\text{C}$, $x_B=0.64$). Upon optimization, most liquidus data proved to lie rather low to be consistent with the reported eutectic temperature. The phase diagram, Fig. 53, was calculated with the use of Eq. (123)

$$G^E(l) = -2088x_A x_B \text{ J mol}^{-1} \quad (123)$$

and the calculated eutectic is $141.0\text{ }^\circ\text{C}$, $x_B=0.619$. An uncertainty of $\pm 3^\circ$ may be assigned to the calculated diagram.

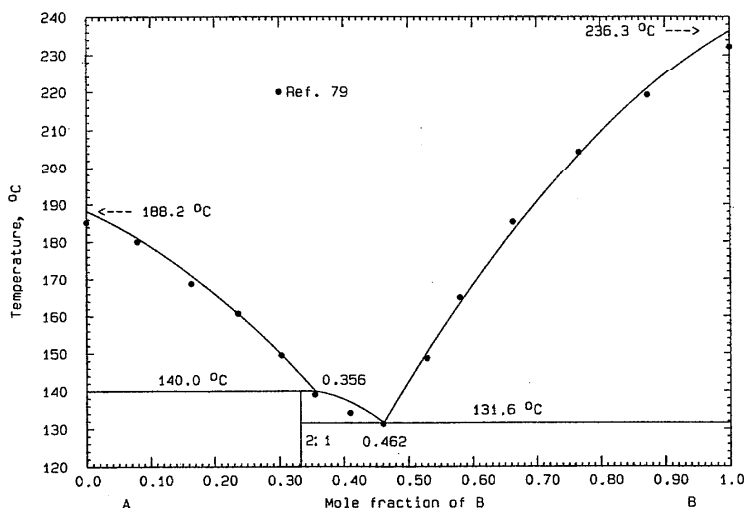


FIG. 54. The system 4-aminobenzoic acid (A)+caffeine (B).

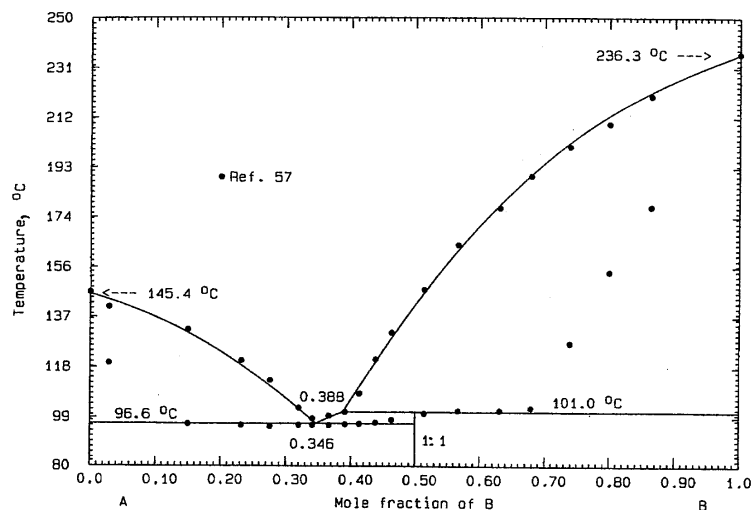


FIG. 55. The system anthranilic acid (A)+caffeine (B).

12.54. 4-Aminobenzoic Acid (A)+Caffeine (B)

Data were obtained by DTA⁷⁹ and the investigators reported the presence of an incongruently melting 2:1 compound ($P=133^\circ\text{C}$, $E=128^\circ\text{C}$). There was a metastable eutectic at 116°C . A 1:1 compound,¹⁰⁷ isolated from aqueous solution, melted at $70\text{--}71^\circ\text{C}$. The data could be well represented by

$$G^E(l) = -6644x_Ax_B \quad \text{J mol}^{-1} \quad (124)$$

for the liquid and

$$\Delta_{\text{fus}}G^\circ = 10766 - 26.0439T \quad \text{J mol}^{-1}, \quad (125)$$

$$\Delta_f G^\circ = -12242 + 20.7519T \quad \text{J mol}^{-1} \quad (126)$$

for the compound $\Lambda_2B/3$. The calculated phase diagram is shown in Fig. 54 ($P=140.0^\circ\text{C}$, $x_B=0.356$; $E=131.6^\circ\text{C}$, $x_B=0.462$). An uncertainty of $\pm 3^\circ$ may be assigned to the calculated diagram.

12.55. Anthranilic Acid (A)+Caffeine (B)

Data were obtained by the thaw-melt method on physical and fused mixtures⁵⁷ (only data from fused mixtures are shown on the diagram). There is a 1:1 compound melting incongruently and a metastable eutectic at $\sim 89^\circ\text{C}$. All the liquidus data for fused mixtures were optimized to give

$$G^E(l) = x_Ax_B(-8146 - 2330x_B + 4918x_B^2) \quad \text{J mol}^{-1} \quad (127)$$

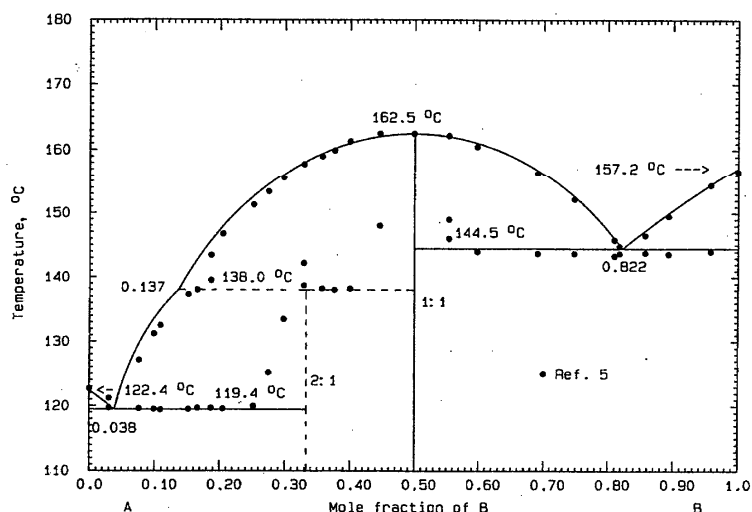


FIG. 56. The system benzoic acid (A)+isonicotinamide (B). The existence of the 2:1 compound is debatable.

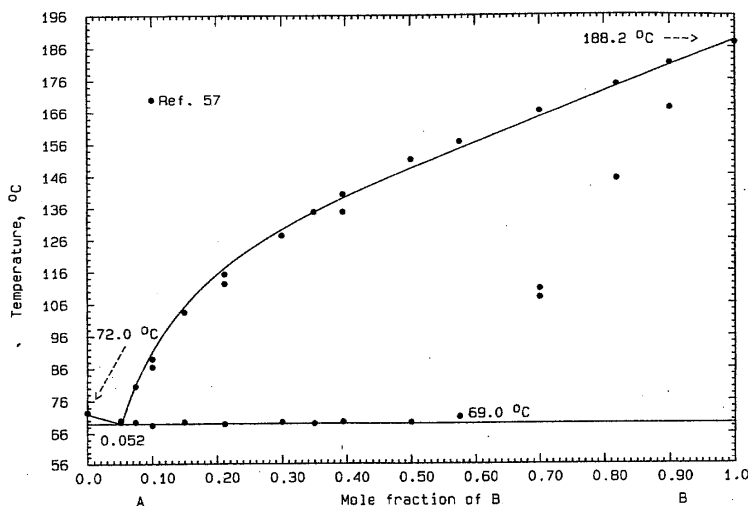


FIG. 57. The system 2-nitroaniline (A)+4-aminobenzoic acid (B).

for the liquid and

$$\Delta_{\text{fus}}G^{\circ} = 15\,544 - 41.0043T \quad \text{J mol}^{-1}, \quad (128)$$

$$\Delta_{\text{f}}G^{\circ} = -17\,564 + 35.2415T \quad \text{J mol}^{-1} \quad (129)$$

for the compound AB/2. The calculated phase diagram is shown in Fig. 55, with calculated data $E=96.6^{\circ}\text{C}$, $x_{\text{B}}=0.346$ and $P=101.0^{\circ}\text{C}$, $x_{\text{B}}=0.388$. An uncertainty of $\pm 2^{\circ}$ may be assigned to the calculated diagram.

12.56. Benzoic Acid (A)+Isonicotinamide (B)

Data were obtained by the thaw-melt method.⁵ There is a congruently melting 1:1 compound, and a metastable eutectic at $\sim 115^{\circ}\text{C}$. Thermal activity in the range $0.25 < x_{\text{B}} < 0.5$ suggested the presence of another compound, possibly

2:1 (incongruent). This may be a metastable compound. In preliminary calculations, it was ascertained that the expressions

$$G^E(l) = -1712x_{\text{A}}x_{\text{B}} \quad \text{J mol}^{-1} \quad (130)$$

for the liquid and

$$\Delta_{\text{fus}}G^{\circ} = 26\,822 - 61.5704T \quad \text{J mol}^{-1}, \quad (131)$$

$$\Delta_{\text{f}}G^{\circ} = -27\,250 + 55.8092T \quad \text{J mol}^{-1} \quad (132)$$

for the compound AB/2 could establish the RHS eutectic and the melting point of the 1:1 compound quite accurately. The LHS eutectic temperature could be reproduced with the presence of the 2:1 compound, whose assigned (not optimized) properties are

$$\Delta_{\text{fus}}G^{\circ} = 27\,334 - 65.2920T \quad \text{J mol}^{-1}, \quad (133)$$

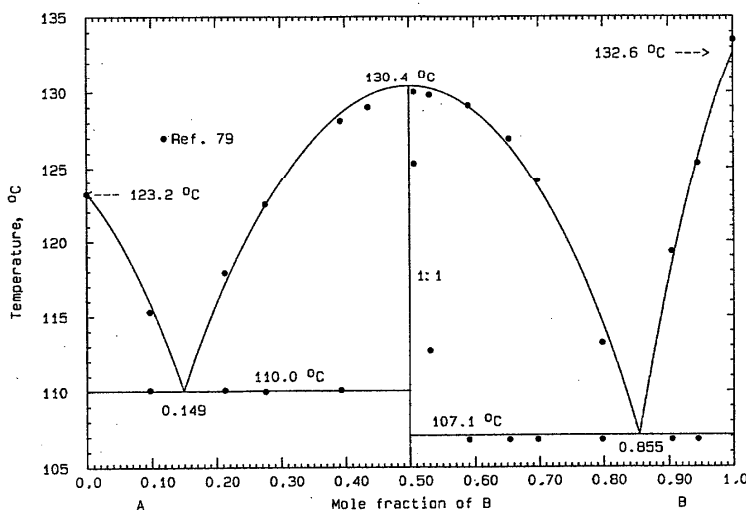


FIG. 58. The system succinimide (A)+urea (B).

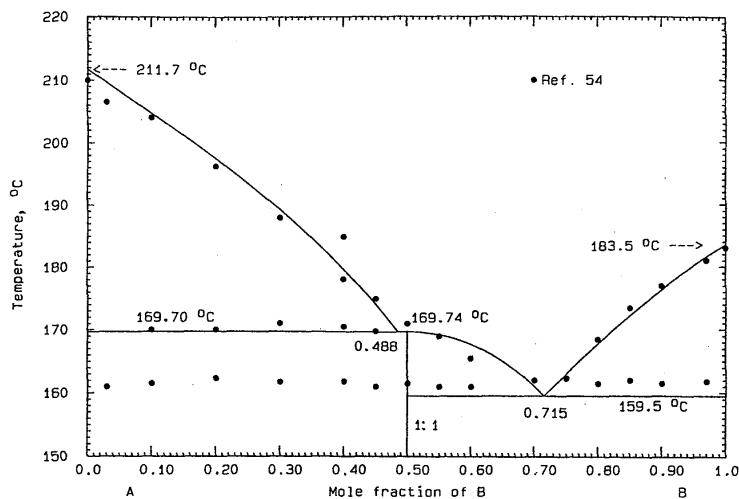


Fig. 59. The system chlormadinone acetate (A)+ethinyl estradiol (B).

$$\Delta_f G^\circ = -27714 + 60.0000T \quad \text{J mol}^{-1} \quad (134)$$

for $A_2B/3$. The final calculated phase diagram is shown in Fig. 56. The calculated eutectics are $E_1 = 119.4^\circ\text{C}$, $x_B = 0.038$ and $E_2 = 144.5^\circ\text{C}$, $x_B = 0.822$. The 1:1 compound melts at 162.5°C . The calculated peritectic is 138.0°C , $x_B = 0.137$. The properties of the 2:1 compound, Eq. (133) and (134), are of reasonable magnitude, but there is doubt about its existence. An uncertainty of $\pm 2^\circ$ may be assigned to the calculated diagram.

12.57. 2-Nitroaniline (A)+4-Aminobenzoic Acid (B)

Data were obtained by the thaw-melt method⁵⁷ on physical, fused and solvent-evaporated mixtures (only data from fused and solvent-evaporated mixtures are shown in the phase diagram). No invariant points were stated. All liquidus data were optimized to give

$$G^E(l) = x_A x_B (2987 - 1112x_B) \quad \text{J mol}^{-1} \quad (135)$$

and the phase diagram calculated with this expression is shown in Fig. 57. The calculated eutectic is 69.0°C , $x_B = 0.052$. An uncertainty of $\pm 2^\circ$ may be assigned to the calculated diagram.

12.58. Succinimide (A)+Urea (B)

Data were obtained by DTA,⁷⁹ and the reported eutectic temperatures are 110 and 107°C . There is a congruently melting 1:1 compound. The data were fitted well by the expression

$$G^E(l) = x_A x_B (-15750 - 2000x_B) \quad \text{J mol}^{-1} \quad (136)$$

for the liquid and

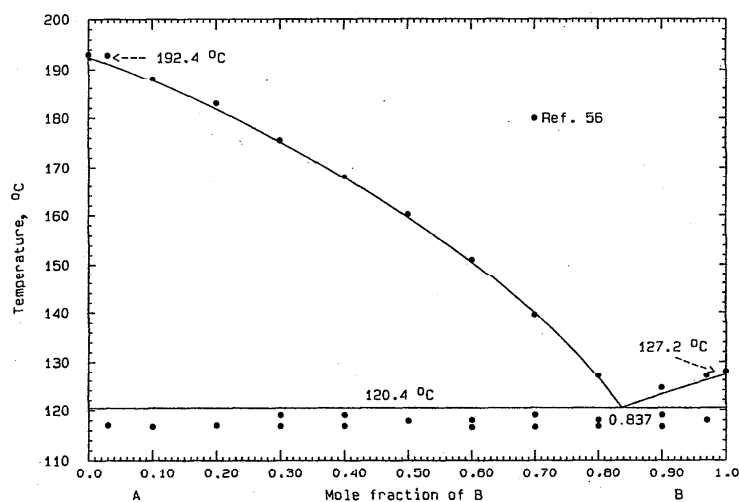


Fig. 60. The system estradiol benzoate (A)+estradiol phenylpropionate (B).

$$\Delta_{\text{fus}}G^{\circ} = 58\,863 - 145.8652T \quad \text{J mol}^{-1}, \quad (137)$$

$$\Delta_{\text{f}}G^{\circ} = -63\,051 + 140.1040T \quad \text{J mol}^{-1} \quad (138)$$

for the compound AB/2. The calculated diagram is shown in Fig. 58 and calculated data are $E_1 = 110.0^{\circ}\text{C}$, $x_B = 0.149$ and $E_2 = 107.1^{\circ}\text{C}$, $x_B = 0.855$. The compound melts at 130.4°C . The excess Gibbs energy of the liquid, Eq. (136), is very negative and the entropy of fusion of the compound, Eq. (137), is rather large compared to other systems examined in this work. Nevertheless the experimental data are faithfully reproduced. An uncertainty of $\pm 1^{\circ}$ may be assigned to the calculated diagram.

12.59. Chlorzoxiprone Acetate (A)+Ethinyl Estradiol (B)

Data were obtained by DSC, light transmission and thermal microscopy.⁵⁴ The results of these three methods are concordant. The presence of a 1:1 compound was confirmed by x-ray diffraction on solid samples, as well as by photomicrographic examination. A peritectic temperature of 170°C and a eutectic 160°C , $x_B = 0.75$ were reported. Thermal events near 140°C were attributed to metastable transitions. From the experimental data it is difficult, if not impossible, to decide whether the compound melts congruently or incongruently. Optimization of the liquidus data resulted in Eq. (139)

$$G^E(l) = x_A x_B (259 - 2426x_B) \quad \text{J mol}^{-1} \quad (139)$$

for the liquid and

$$\Delta_{\text{fus}}G^{\circ} = 20\,004 - 45.1648T \quad \text{J mol}^{-1}, \quad (140)$$

$$\Delta_{\text{f}}G^{\circ} = -20\,292 + 39.4036T \quad \text{J mol}^{-1} \quad (141)$$

for the compound AB/2. The calculated phase diagram is shown in Fig. 59. The compound is shown to melt congruently at 169.74°C , but the E_1 eutectic (169.70°C , $x_B = 0.488$) is so close that the congruency of melting of the compound is still uncertain. On the RHS, $E_2 = 159.5^{\circ}\text{C}$, $x_B = 0.715$. An uncertainty of $\pm 2^{\circ}$ may be assigned to the calculated diagram.

12.60. Estradiol Benzoate (A)+Estradiol Phenylpropionate (B)

Data were obtained by DSC and thermomicroscopy.⁵⁶ The reported eutectic is 118°C , $x_B = 0.85$. This temperature corresponds to thermal arrests from DSC; those from thermal microscopy were slightly lower. The liquidus data from the two methods were generally concordant within 1° . The liquidus data, when optimized, yielded the quantity

$$G^E(l) = x_A x_B (-1825 + 1583x_B) \quad \text{J mol}^{-1} \quad (142)$$

and the phase diagram, calculated by means of this equation, is shown in Fig. 60. The liquidus data are fitted well, and the calculated eutectic is 120.4°C , $x_B = 0.837$. The calculated eutectic temperature is significantly higher than the experimental datum, but is thermodynamically consistent with the

liquidus data. In this case, the liquidus data were taken as the defining data. An uncertainty of $\pm 2^{\circ}$ may be assigned to the calculated diagram.

13. Acknowledgments

Thanks are due to Professor C. W. Bale and Professor A. D. Pelton, Center for Research in Computational Thermochemistry, Ecole Polytechnique de Montréal, for use of computing facilities.

14. References

- J. W. Shell, *J. Pharm. Sci.* **52**, 100 (1963).
- A. Watanabe, Y. Yamaoka, and K. Takada, *Chem. Pharm. Bull.* **30**, 2958 (1982).
- M. Kuhnert-Brandstätter, *Thermomicroscopy in the Analysis of Pharmaceuticals* (Pergamon, Oxford, 1985).
- J. K. Guillory, S. C. Hwang, and J. L. Lach, *J. Pharm. Sci.* **58**, 301 (1969).
- K. Sekiguchi, I. Himuro, I. Horikoshi, T. Tsukada, T. Okamoto, and T. Yotsuyanagi, *Chem. Pharm. Bull.* **17**, 191 (1969).
- C. Caramella, F. Giordano, G. P. Bettinetti, P. Colombo, and U. Corte, *Farmaco Ed. Prat.* **35**, 277 (1980).
- W. N. French and J. C. Morrison, *J. Pharm. Sci.* **54**, 1133 (1965).
- D. J. W. Grant, H. Jacobson, J. E. Fairbrother, and C. G. Patel, *Int. J. Pharm.* **5**, 109 (1980).
- K. Sekiguchi and K. Ito, *Chem. Pharm. Bull.* **13**, 405 (1965).
- G. Bettinetti and F. Giordano, *Drug Dev. Ind. Pharm.* **14**, 431 (1988).
- A. G. Eshra, V. F. Naggar, and N. A. Boraie, *Pharm. Ind.* **48**, 1557 (1986).
- H. M. El-Banna, S. Abd-Elfattah, and N. A. Daabis, *Pharmazie* **29**, 396 (1974).
- H. Wollmann and V. Braun, *Pharmazie* **38**, 5 (1983).
- E. E. Marti, *Thermochemica Acta* **5**, 173 (1972).
- J. Sangster and A. D. Pelton, *J. Phys. Chem. Ref. Data* **16**, 509 (1987).
- J. Sangster, P. K. Talley, C. W. Bale, and A. D. Pelton, *Can. J. Chem. Eng.* **66**, 881 (1988).
- J. Sangster, *J. Phys. Chem. Ref. Data* **23**, 295 (1994).
- P. Wu and A. D. Pelton, *J. Alloys Comp.* **179**, 259 (1992).
- J. Sangster, *J. Phase Equil.* **14**, 340 (1993).
- A. D. Pelton, "Phase Diagrams," Eds., *Physical Metallurgy*, Chap. 2, 3rd ed., edited by R. W. Cahn and P. Haasen (North-Holland, New York, 1981).
- J. Jacques, A. Collet, and S. H. Wilen, *Enantiomers, Racemates and Resolutions* (Wiley-Interscience, New York, 1981).
- W. T. Thompson, C. W. Bale, and A. D. Pelton, F*A*C*T (Facility for the Analysis of Chemical Thermodynamics). Programs FITBIN and POTCOMP (McGill University, Montreal, 1985).
- E. E. Marti, *J. Thermal Anal.* **33**, 37 (1988).
- J. Wisniak, *Phase Diagrams: A Literature Source Book* (Elsevier, New York, 1981/1986), Vols. I and II.
- Dictionary of Organic Compounds*, 6th ed., edited by J. Buckingham and F. MacDonald (Chapman and Hall, London, 1996).
- The Merck Index*, 12th ed., edited by S. Budavari (Merck and Company, Whitehouse Station, 1996).
- J. Elks and C. R. Ganellin, *Dictionary of Drugs* (Chapman and Hall, London, 1990), Vols. I and II.
- Handbook of Chemistry and Physics*, 73rd ed., edited by D. R. Lide (Chemical Rubber Corp., Boca Raton, FL, 1992).
- Heat Capacities and Entropies of Organic Compounds*, 2nd ed., edited by R. C. Weast and J. G. Grasselli (Chemical Rubber Corp., Boca Raton, FL, 1989).
- E. S. Domalski and E. D. Hearing, *J. Phys. Chem. Ref. Data* **25**, 1 (1996).
- W. E. Acree, in Ref. 28, pp. 5-97.
- L. T. Grady, S. E. Hays, R. H. King, H. R. Klein, W. J. Mader, D. K. Wyatt, and E. O. Zimmerer, *J. Pharm. Sci.* **62**, 456 (1973).
- R. J. L. Andon and J. E. Connett, *Thermochem. Acta* **42**, 241 (1980).

- ³⁴ J. E. Connett, *J. Calorim. Therm. (Prepr.)* **10**, E1.1 (1979).
- ³⁵ D. Giron-Forest, C. Goldbloom, and P. Piechon, *J. Pharm. Pharmacol.* **7**, 1421 (1989).
- ³⁶ M. Macy and M. A. Valerdi, *Mater. Chem. Phys.* **8**, 259 (1983).
- ³⁷ A. A. Van Dooren and B. W. Müller, *Thermochim. Acta* **66**, 161 (1983).
- ³⁸ C. Treiner, C. Vaution, and G. N. Cave, *J. Pharm. Pharmacol.* **34**, 538 (1986).
- ³⁹ A. Chauvet, G. De Maury, A. Terol, and J. Masse, *Thermochim. Acta* **97**, 143 (1986).
- ⁴⁰ W. E. Acree, *Thermochim. Acta* **189**, 37 (1991).
- ⁴¹ H.-M. Lin and R. A. Nash, *J. Pharm. Sci.* **82**, 1018 (1993).
- ⁴² J. Masse and A. Chauvet, *J. Thermal Anal.* **14**, 313 (1978).
- ⁴³ A. Terol, A. Chauvet, and G. De Maury, *J. Thermal Anal.* **32**, 1253 (1987).
- ⁴⁴ A. Chauvet, R. Malaviolle, and J. Masse, *Trav. Soc. Pharm. Montpellier* **37**, 217 (1977).
- ⁴⁵ J. Masse and A. Chauvet, *Talanta* **26**, 1019 (1979).
- ⁴⁶ J. Masse and A. Chauvet, *J. Thermal Anal.* **14**, 299 (1978).
- ⁴⁷ E. Fukuoka, M. Makita, and S. Yamamura, *Chem. Pharm. Bull.* **37**, 1047 (1989).
- ⁴⁸ K. Nikolics, S. Gál, J. Sztatiz, and K. Nikolics, *Acta Pharm. Hung.* **46**, 205 (1976).
- ⁴⁹ U. S. Rai and S. George, *Cryst. Res. Technol.* **26**, 511 (1991).
- ⁵⁰ S. H. Neau and G. L. Flynn, *Pharm. Res.* **7**, 1157 (1990).
- ⁵¹ G. P. Bettinetti, C. Caramella, F. Giordano, A. La Manna, C. Margheritis, and C. Sinistri, *J. Thermal Anal.* **28**, 285 (1983).
- ⁵² B. L. Sharma, N. K. Sharma, and M. Rambal, *Thermochim. Acta* **206**, 71 (1992).
- ⁵³ P. V. Babilev and V. V. Chiripitko, *Farm. Zh. (Kiev)* **2**, 61 (1985).
- ⁵⁴ G. De Maury, A. Chauvet, A. Terol, and J. Masse, *Thermochim. Acta* **89**, 203 (1985).
- ⁵⁵ G. De Maury, A. Chauvet, and J. Masse, *Thermochim. Acta* **87**, 189 (1985).
- ⁵⁶ G. De Maury, A. Terol, and J. Masse, *J. Thermal Anal.* **32**, 121 (1987).
- ⁵⁷ K. Sekiguchi, Y. Ueda, and Y. Nakamori, *Chem. Pharm. Bull.* **11**, 1108 (1963).
- ⁵⁸ P. Bret-Dibat and A. Lichanot, *Thermochim. Acta* **147**, 261 (1989).
- ⁵⁹ N. G. Buckman, J. O. Hill, and R. G. Magee, *J. Thermal Anal.* **37**, 79 (1991).
- ⁶⁰ W. E. Acree, *Thermochim. Acta* **219**, 97 (1993).
- ⁶¹ Z. Galdecki, M. L. Glowka, and Z. Górkiewicz, *Acta Polon. Pharm.* **34**, 521 (1977).
- ⁶² M. Draguet-Brughmans and R. Bouché, *J. Thermal Anal.* **20**, 141 (1981).
- ⁶³ N. Kaneniwa, M. Otsuka, and T. Hayashi, *Chem. Pharm. Bull.* **33**, 3447 (1985).
- ⁶⁴ J. Masse, R. Malaviolle, and A. Chauvet, *J. Thermal Anal.* **16**, 123 (1979).
- ⁶⁵ J. Masse, R. Malaviolle, and A. Chauvet, *J. Thermal Anal.* **16**, 341 (1979).
- ⁶⁶ A. Chauvet, A. Terol, G. De Maury, R. Malaviolle, and J. Masse, *Thermochim. Acta* **147**, 217 (1989).
- ⁶⁷ R. Malaviolle, G. De Maury, A. Chauvet, A. Terol, and J. Masse, *Thermochim. Acta* **121**, 283 (1988).
- ⁶⁸ M. S. L'vova, N. I. Garber, and E. I. Kozlov, *J. Thermal Anal.* **33**, 1231 (1988).
- ⁶⁹ R. Palepu and L. Moore, *Thermochim. Acta* **30**, 384 (1979).
- ⁷⁰ R. Sabbah and M. Gouali, *Aust. J. Chem.* **47**, 1651 (1994).
- ⁷¹ J. R. Donnelly, L. A. Drewes, R. L. Johnson, W. D. Munslow, K. K. Knapp, and G. W. Sovocool, *Thermochim. Acta* **167**, 155 (1990).
- ⁷² B. Jeanjean, S. Alberola, A. Terol, F. Sabon, and B. Pauvert, *Ann. Pharm. Fr.* **37**, 95 (1979).
- ⁷³ S. V. Gritsenko, G. M. Dugacheva, N. V. Avramenko, L. I. Brutko, and A. G. Anikin, *Khim.-Farm. Zh.* **12**, 101 (1978).
- ⁷⁴ G. M. Gustin, *Thermochim. Acta* **39**, 81 (1980).
- ⁷⁵ F. I. Khattab, *Thermochim. Acta* **61**, 253 (1983).
- ⁷⁶ B. Jeanjean, S. Alberola, J. Rambaud, F. Sabon, and B. Pauvert, *Ann. Pharm. Fr.* **37**, 175 (1974).
- ⁷⁷ N. Kaneniwa, J.-I. Ichikawa, and T. Matsumoto, *Chem. Pharm. Bull.* **36**, 1063 (1988).
- ⁷⁸ M. D. Tuladhar, J. E. Carless, and M. P. Summers, *J. Pharm. Pharmacol.* **35**, 208 (1983).
- ⁷⁹ K. Sekiguchi, I. Himuro, I. Horikoshi, T. Tsukada, T. Okamoto, and T. Yotsuyanagi, *Chem. Pharm. Bull.* **17**, 191 (1969).
- ⁸⁰ G. G. Lobbia, G. Berchiesi, and G. Poeti, *Thermochim. Acta* **78**, 297 (1984).
- ⁸¹ S. S. Yang and J. Guillory, *J. Pharm. Sci.* **61**, 26 (1972).
- ⁸² J. Masse, R. Malaviolle, and A. Chauvet, *Ann. Pharm. Fr.* **34**, 407 (1976).
- ⁸³ F. Giordano and G. P. Bettinetti, *J. Pharm. Biomed. Anal.* **6**, 951 (1988).
- ⁸⁴ C. Sunwoo and H. Eisen, *J. Pharm. Sci.* **60**, 238 (1971).
- ⁸⁵ J. Rambaud, B. Pauvert, Y. Lasserre, and M. Audran, *Farmaco Ed. Prat.* **41**, 26 (1986).
- ⁸⁶ F. Giordano, G. P. Bettinetti, A. La Manna, and P. Ferloni, *Farmaco Ed. Sci.* **32**, 889 (1977).
- ⁸⁷ L. Maury, J. Rambaud, B. Pauvert, G. Berge, M. Audran, and Y. Lasserre, *Pharm. Acta Helv.* **60**, 22 (1985).
- ⁸⁸ J. Rambaud, L. Maury, Y. Lasserre, G. Berge, M. Audran, and J. P. Declercq, *Farmaco Ed. Prat.* **40**, 152 (1985).
- ⁸⁹ G. Siracusa and L. Abate, *Thermochim. Acta* **36**, 207 (1980).
- ⁹⁰ L. Vogel and H. Schuberth, *Chem. Tech. (Leipzig)* **32**, 143 (1980).
- ⁹¹ O. A. Momot, I. A. Borukhov, and M. T. Saibova, *Deposited Document VINITI 2964-76* (1976), 6 pp.
- ⁹² A. A. Kozyro, S. V. Dalidovich, and A. P. Krasulin, *Zh. Prikl. Khim. (Leningrad)* **59**, 1456 (1986).
- ⁹³ T. Ozawa, *Thermochim. Acta* **92**, 27 (1985).
- ⁹⁴ K. G. Joback and R. C. Reid, *Chem. Eng. Commun.* **57**, 233 (1987).
- ⁹⁵ K. Mislow, *J. Phys. Colloid Chem.* **52**, 729 (1948).
- ⁹⁶ A. Bylicki, *Bull. Acad. Pol. Sci., Ser. Sci. Chim., Géol., Géogr.* **7**, 239 (1959).
- ⁹⁷ H. Rheinboldt and E. B. Berthold, *Univ. Sao Paulo, Fac. Filos. Cienc. Let., Ouim.* **2**, 105 (1947).
- ⁹⁸ K. Hrynakowski and F. Adamanis, *Bull. Soc. Chim. Fr.* **53**, 1168 (1933).
- ⁹⁹ T. Gondova, P. Kralik, and J. Gonda, *Thermochim. Acta* **156**, 147 (1989).
- ¹⁰⁰ G. M. Dugacheva, L. A. Saryan, and V. A. Popkov, *Vestn. Mosk. Univ., Ser. 2: Khim.* **32**, 246 (1991).
- ¹⁰¹ G. Giuseppetti, C. Tadani, G. P. Bettinetti, F. Giordano, and A. La Manna, *Farmaco Ed. Sci.* **35**, 138 (1980).
- ¹⁰² A. J. Winfield and S. M. H. Al Saidan, *Int. J. Pharm.* **8**, 211 (1981).
- ¹⁰³ A. M. Agrawal, K. L. Nikore, and A. K. Dorle, *Indian J. Pharm.* **35**, 41 (1973).
- ¹⁰⁴ V. Ariescu, C. Ionescu, A. Tilinca, Z. Cojocar, and M. Pitea, *Farmacia (Bucharest)* **9**, 65 (1961).
- ¹⁰⁵ W. M. Higgins and M. F. W. Dunker, *J. Am. Pharm. Ass., Sci. Ed.* **33**, 310 (1944).
- ¹⁰⁶ H. Busquet and C. Vischniac, *Compt. Rend. Soc. Biol.* **119**, 503 (1935).
- ¹⁰⁷ T. Higuchi and J. L. Lach, *J. Am. Pharm. Assoc., Sci. Ed.* **43**, 349 (1954).
- ¹⁰⁸ S. Alberola, J. Rambaud, B. Jeanjean, and F. Sabon, *Trav. Soc. Pharm. Montpellier* **36**, 281 (1976).
- ¹⁰⁹ N. A. Daabis, S. Abd-Elfattah, and H. M. El-Banna, *Pharmazie* **29**, 396 (1974).
- ¹¹⁰ R. Malviolle, G. De Maury, A. Chauvet, A. Terol, and J. Masse, *J. Calorim., Anal. Therm. Thermodyn. Chim.* **17**, 497 (1986).